University Of Jordan

Faculty Of Graduate Studies

NEW MATHEMATICAL
ANALYTICAL METHOD
FOR SOLVING
PHASE-CHANGE PROBLEMS

BY

FAWZIE YOUSEF EID ELWERR

UNDER THE SUPERVISION OF

DR. MOHAMMAD A. HAMDAN

عميد كلية الدراسات العليا

Submitted in partial fulfillment of the requirements for the degree

of Master of Science in Mechanical Engineering.

Faculty of Graduate Studies,

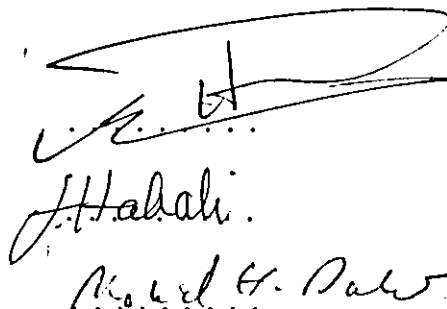University of Jordan

Amman, Jordan

August, 1993

This thesis was defended successfully on 28/8/1993.

COMMITTEE MEMBERS   SIGNATURE

1. Dr. Mohammad A. Hamdan

2. Dr. Saad M. Habali

3. Dr. Mohammad H. Aldado

ACKNOWLEDGEMENTS

With deep pleasure I express my gratitude to all who helped me during the preparation and completion of this work, especially my supervisor, Dr Mohammad A. Hamdan, who without his support, and advice, my work could have been more difficult. Also, I have to mention the encouragement offered to me by my family and my friends.

Contents

NOMENCLATURE

A : aspect ratio of the enclosure, H/B

B : enclosure width, m

H : enclosure height, m

D : enclosure depth, m

c : specific heat of PCM, J/Kgc^o

F : melted fraction of phase change material, (PCM)

f : a proportional constant for ϕ vs τ

G : heat gain stored inside the enclosure, MJ

$\hat{G}$: dimensionless gain, $GRa^{1/5}/H^2\rho_l Q_{sl}$

g : acceleration due to gravity, m/s^2

h : coefficeint of convective heat transfer, W/m^2c^o

$\hat{h}$: dimensionless coefficient, hH/K_l

k : thermal conductivity of PCM, W/mc^o

m : a constant, see equation (4-26)

n : a constant, see equation (4-25)

Nu : Nusselt number, hy/k

$p(B,H)$: RHS top corner of the enclosure

Pr : Prandtl number of PCM, ν/α

Q_{sl} : latent heat of fusion of PCM, J/Kg

q : heat flux, W/m^2

$\hat{q}$: dimensionless heat flux, $qH/K_l\Delta_{wm}$

Ra : Rayleigh number, $g\beta\Delta_{wm}H^3/\nu\alpha$

S : local melted layer thickness, m

$\hat{S}$: dimensionless thickness, $SRa^{1/5}/H$

S_0 : melted layer thickness at the bottom, m

Ste : Stefan number, $c_l\Delta_{wm}/Q_{sl}$

t : dimensional time, $seconds$

T : temperature, c^o

u : horizontal (or lateral) component of liquid velocity, m/s

$\hat{u}$: dimensionless velocity, $uH/\alpha_l Ra^{1/5}$

v : vertical (or longitudinal) component of liquid velocity, m/s

V : local characteristic velocity, m/s

x : horizontal (or lateral) coordinate

$\hat{x}$: dimensionless coordinate, x/H

y : vertical (or longitudinal) coordinate

$\hat{y}$: dimensionless coordinate, y/H

Y : coordinate defined in equation (4-29)

$\hat{Y}$: dimensionless coordinate, Y/H

GreekSymbols :

α :	thermal diffusivity of PCM, m^2/s
β :	volume expansivity of liquid phase of PCM, $1/c^o$
Δ :	dimensional temperature difference, c^o
$\hat{\Delta}$:	dimensionless difference, $\Delta Ra^{1/5}/\Delta_{wm}$
Δ_{wl} :	temperature difference, $(T_w - T_l)$, c^o
Δ_{wm} :	temperature difference, $(T_w - T_m)$, c^o
Δ_{lm} :	temperature difference, $(T_l - T_m)$, c^o
$\Delta_{l'm}$:	temperature difference, $(T_{l'} - T_m)$, c^o
Δ_{mi} :	temperature difference, $(T_m - T_i)$, c^o
δ :	boundary layer thickness, m
$\hat{\delta}$:	dimensionless thickness, $\delta Ra^{1/5}/H$
λ :	proportionality parameter of S_0 vs t
ν :	kinematic viscosity of PCM, m^2/s
ρ :	density of PCM, Kg/m^3
τ :	dimensionless time, $\alpha_l Ra^{2/5}t/H^2$
τ_0 :	dimensionless time of the conduction stage
ϕ :	inclination angle of solid-liquid interface, *radians*
$\hat{\phi}$:	dimensionless inclination angle, $\phi Ra^{1/5}$
ϕ_B :	value of ϕ when the interface contacts point $p(B,H)$

Subscripts :

a :	'after' the interface contacts point $p(B,H)$
av :	average
b :	'before' the interface contacts point $p(B,H)$
c :	cold boundary layer
h :	hot boundary layer
i :	initial conditions
l :	liquid core along the vertical y-coordinate
l' :	liquid core along the inclined y'-coordinate
m :	melting
r :	ratio of solid to liquid properties
s :	solid phase
t :	total
w :	vertical heated wall

Superscripts :

$'$:	refers to l' and (x',y') coordinate system
$\hat{}$:	nondimensionlization symbol

Othersymbols :

PCES :	Phase-Change Energy Storage
PCMs :	Phase Change Materials
TES :	Thermal Energy Storage

List of Figures

ABSTRACT

In this work, two-dimensional melting process of a solid phase change material contained in a rectangular enclosure heated from a vertical isothermal side, while all its other sides are insulated, is investigated analytically. During the early stages of the melting process, it is considered that the heat transfer in the liquid phase is controlled by the conduction mode, followed by a short transition period after which, the natural convection is considered to be the predominant mode of heat transfer in the liquid phase until the end of the melting process. The solid-liquid interface time-dependent inclination, during the natural convection regime, is taken into account, whose propagation at the bottom of the enclosure is considered to be conduction-controlled during the whole melting process, while the propagation and inclination of the rest of the interface is considered to be convection-controlled during the convection regime. Two boundary layers, seperated by a stationary liquid core, a hot one adjacent to the vertical heatad wall, and a cold one adjacent to the solid-liquid interface, are analysed. Temperature and velocity distributions and the mass conservation for the two boundary layers are evaluated. The governing equations for the whole process are solved and an analytical solution is developed. Experimental and numerical matrixes of selected previous works are substituted in corresponding equations developed in this work, results are obtained and found to be in good agreement with results of those works concerning the position, inclination and propagation of the solid-liquid interface and the melted fraction. Finally, using the developed solution in this work, phase change energy storage in rectangular enclosures is investigated.

Chapter 1

INTRODUCTION

1.1 Phase-Change Problems

Many problems arise in engineering in which heat transfer is accompanied by a change of phase with release or absorption of thermal energy. Notable examples of this phenomena are the melting and solidification process in which a sharp moving interface separates between two regions of different thermophysical properties; namely the liquid and the solid phases. The displacement, shape and position of the solid-liquid interface are time-dependent, accordingly, the shape and dimensions of the two phases vary with time. At the interface, the thermal energy is liberated during solidification process and absorbed during melting process.

Such transient heat transfer problems are referred to as 'phase- change', 'moving-boundary' or, sometimes, 'Stefan' problems. The recent years have witnessed an upsurge of published works dealing with these problems.

1.2 Importance And Applications Of Phase Change Problems

Melting and solidification phase change problems have found considerable attention from mathematicians, engineers and scientists alike in the recent past as these problems arise in many industrial, residential and applied science processes. Some applications of these problems are:

1. Formation of ice.

2. Controlled melting and casting of metals.

3. Welding.

4. Synthetic production of alloys.

5. Growth of pure crystals.

6. Cooling of igneous rocks.

7. Purification of materials.

8. Freeze and drying of foodstuffs.

9. Controlled ablation of thermal shield in aerospace engineering.

10. Bioengineering cryopreservation of tissues.

11. Latent heat of fusion energy storage.

Recently, attention has been given to the use of Phase Change Energy Storage (PCES) in residential solar heating and cooling systems and in industrial processing. Recent studies [1,2] have shown that the PCES offers significant advantage over sensible storage of thermal energy. Several previous works [2,3,4,5,6,7,8,9] were motivated by the need for basic informations required to predict the position of the solid- liquid interface, which is essential in designing PCES systems. Commercial acceptance of economics of solar energy, energy conservation, waste heat utilization and other alternate energy technologies is directed towards the design and development of efficient and cost-effective Thermal Energy Storage (TES) systems. Among the possible application of the TES systems, interest has been focused on the use of a latent-heat solar walls in passive solar heating of homes [7]. These proposed walls consist of rectangular enclosures filled with a Phase Change Material (PCM) and are subject to heating through their vertical surfaces by direct exposure to solar irradiation. Other interests [1,6,10] were about using systems consisting of conventional solar collectors connected to sub-systems of latent-heat storage heat exchangers.

different values of melting temperatures makes these systems suitable to be used in different types of applications.

The objectives of this work are:

1. To develop a relatively simple analytical solution for the melting process of a PCM contained in a rectangular enclosure heated from a vertical isothermal wall so as to be used to predict the melting rate and all the other data related to the melting process throughout few simple analytical steps compared to the costly complicated long procedure of the experimental and numerical methods.

2. To demonstrate the degree of efficiency and accuracy of this developed solution by comparing the results obtained in this work with the results obtained by selected previous experimental and numerical works.

3. To establish a fundamental understanding of heat transfer during the whole melting process of a PCM to find out the effects of different parameters on the efficient design of a PCES system.

4. To use the developed analytical solution in order to predict the amount of TES within a rectangular enclosure filled with PCM and is subject to isothermal heating from vertical side.

This work consists of six chapters in which this chapter is the first. Literature survey is conducted in chapter II. Description of the employed model in this work, physical analysis of the melting process and mathematical formulation of the problem are presented in chapter III. Melting of a PCM contained in a rectangular enclosure heated from its vertical isothermal wall is investigated mathematically and the analytical solution is developed in chapter IV. The discussion of the obtained results and comparing them with experimental and numerical results of previous works are presented in chapter V. The conclusions and recommendations are found in chapter VI.

Chapter 2

LITERATURE REVIEW

2.1 Introduction

Early analytical works on solution of phase change problems include those published by Lame' and Clapeyron (1831) and by Stefan (1891) who studied the thickness and formation of the polar ice [20,22]. More recently much attention has been directed towards the ablation of materials as a protective device in the design of atmospheric reentry vehicles. Because of nonlinearity of governing equations of these problems, exact analytical solutions can be developed only for a limited number of specific idealized situations involving semi-infinite or infinite regions and subject to simple boundary and initial conditions. An exact solution of a problem describing a semi-infinite one-dimensional slab, initially at a uniform temperature, was discussed by Neumann in his lectures in (1860) which were published in (1912) [20]. In the first place, solutions of phase change problems are based on pioneer works in conduction heat transfer like those of Fourier (1822) [23,24,25,26], and in convection heat transfer like those of Reynolds, Rayleigh, Nusselt, Blasius and Pohlhausen in early 1900's [27,28,29,30,31,32]. An extensive review article presented by Ostrach (1972) about natural convection heat transfer of liquids in enclosure was of great advantage for solutions of phase change problems throughout the last two decades. Despite their obvious practical value, problems involving melting and solidification have not received their share of attention in heat transfer text books; however, a limited number of such books exist like that of Eckert [22] in which exact and approximate solutions for conduction- controlled heat transfer during melting process are introduced, as

well as those presented by Ozisik [20]. In general, due to the complex mathematical nature of phase change problems, particularly with taking natural convection mode of heat transfer into consideration, the majority of studies avoided analytical solutions and dealt with phase change problems through numerical and experimental methods. Previous works are classified into three groups in the following sections; experimental, numerical and analytical works.

2.2 Experimental Works

The majority of experimental works about phase change problems involving melting and solidification employed n-octadecane paraffin wax as a low melting temperature test-PCM, while fewer works reported about other materials.

Melting of sodium nitrate ($T_m = 244°c$) was investigated by Sparrow et al [11] and was recommended to be used as an intermediate medium in TES systems. Conclusive evidence of natural convection predominance on heat transfer during the melting process was provided by Hale and Viskanta [12] in their photographic observations by demonstrating convection-affected shape, inclination and curvature of the solid-liquid interface during melting of n-octadecane ($T_m = 28°c$) contained in a transparent epexiglass rectangular cell. Similar evidence was presented by Bathelt and Viskanta [4] and Hirata and Nishada [33] in their observations about the unsymmetry of the melt zone around a heat source in a form of horizontal cylinder embedded in n-heptadecane paraffin wax ($T_m = 22°c$) contained in a cylindrical glass cell. During melting process of n-heptadecane, the thermal stratification of the liquid core in forms of horizontal isotherms was shown in interferograms recorded by Buren and Viskanta [13] on camera films using laser beams while the corresponding values of the isotherms were measured by interferometers. The transition from natural convection-controlled to conduction-controlled solidification of n-eicosane paraffin wax ($T_m = 36°$) contained in a rectangular cell cooled from side was studied by Sparrow et al [14] where the solid-liquid interface was found to be straight and vertical which was an indication to the predominance of the conduction mode on the heat transfer during the solidification process.

Figure 2.1 shows a solar PCES collection system proposed by Benard et al [5] which consisted of paraffin wax tanks ($T_m = 60°c$) employed to maintain the room temperature of an experimental chicken brooder within a range of $22°c$ to $30°c$. Encouraging results were obtained and led to construction of other similar units. Figure 2.2 shows another PCES system proposed by the same authors [34] which consisted of latent-heat solar wall filled with paraffin ARCO wax ($T_m = 40/50°c$). A third study was presented by them [15] about melting of n-octadecane in rectangular cells heated from side. Melting process of n-octadecane contained in an internally-finned rectangular cell heated from side was investigated by Henze and Humphery [2] and it was found that the heat transfer coefficient at the heated wall would be doubled by using the appropriate size of fins. As side results, it was reported that the sensible storage accounted for less than 10% of the total TES, and the variation of the thermophysical properties of PCM's over the corresponding range of temperature difference was less than 2% for density, less than 2.5% for specific heat and between 2.6% and 8.5% for thermal conductivity which encouraged to assume these properties to be of constant values in this class of problems.

A shadowgraphic technique was used by Ho and Viskanta [7] to find out the effects convection mode of heat transfer during melting of n- octadecane. Eftekhar et al [8] investigated heat transfer enhancement in a TES system consisting of rectangular cells filled with Suntech P116 paraffin wax ($T_m = 44°c$) heated from below. Okada [35] reported that the solid-liquid interface inclination rate of n-octadecane melting was faster in enclosures of smaller aspect ratio. While Webb and Viskanta [16] found that melting of this PCM was of optimum values for the horizontal position of the enclosure. Due to low thermal conductivity of paraffin wax, it was recommended by Marshal [10] to utilize hybrid water-paraffin wax ($T_m = 55°c$) instead of pure ones in PCES sub-systems assisting solar TES systems as shown in Fig.2.3. Melting of pure gallium ($T_m = 30°c$) contained in rectangular cell heated from side was investigated by Gau and Viskanta [17]. PCES using salt-hydrate ($T_m = 48°c$) was studied by Aboul-Enien and Ramadan [36]

The first two works reported by Zhang and Bejan [9,18] were about melting, with

relatively high Ra numbers (10^{13}), of n-octadecane contained in rectangular cell of large height $(0.75m)$ heated from side at a constant heating rate. The liquid flow during the melting process was weakly turbulent. In their third work [19], published in (1990), solidification of the same PCM was investigated with Ra and Ste numbers of the order of 10^{11} and 0.1 respectively.

2.3   Numerical Works

Compared to experimental works, more numerical works were published about phase change problems involving melting and solidification processes. Also, n-octadecane paraffin wax was employed as test-PCM in most of these works.

An implicit finite-difference solution was used by Sparrow et al [37] for analysis of melting of PCM with a heated vertical tube embedded in this PCM as a heat source and it was found that the greatest thickness of the melt region was at the top of the tube affected by natural convection. Morrison and Abdel-Khalik presented a comparison, of the thermal performance and efficiency, between a PCES system using SUNCO P116 paraffin wax $(T_m = 47^\circ c)$ as PCM and sensible heat storage systems concluding that the selection between the two systems could be decided solely by economic considerations. Goodrich [38] employed Cranck-Nicholson numerical method to solve conduction heat transfer equations of one-dimensional frost. Landau method (1950) was extended by Saitoh [39] to solve multi-dimensional solidification problems in arbitrary geometry. Soloman [3] derived relations via computer simulations for the total melt time and average surface heat flux for PCM enclosed in simple enclosure subject to isothermal side heating. Conduction heat transfer equations during freezing of water were solved numerically by Rubinsky and Cravahlo [40] by applying finite element method recording a formation of $0.25m$ of ice after 80 hours of isothermal cooling at $-20^\circ c$. Similar algorithm and results were obtained by Hsu and Pizey [41]. Boundary immobolization method was used by Hsu et al [42] to obtain numerical results for moving boundary problems. Stefan solidification problem was solved by Gupta and Kumar [21] using a variable time step method.

Similar to his experimental study shown in Fig.2.3, Marshal [6] presented a

study about the use of SHELL $53/54^{o}c$ paraffin wax multiple day PCES in a solar

assisted domestic hot water system and finally he suggested not to replace water by paraffin wax as a TES medium for that application. In their analysis of PCES of n-octadecane in a cylinder capsule, Saitoh and Hirose [43] concluded that the vorticity appearance in the melt layer might be the most important characteristic of melting heat transfer. Numerical prediction of melting propagation speed obtained by Gadgil and Gobin [44] for two dimensional melting of n-octadecane in a rectangular enclosure was 37% larger than that observed experimentally and it was explained to be due to actual heat losses through cell sides. Numerical results obtained by Roa and Sastri [45] for melting in rectangular prisms showed no significance change with varying time step size. Metal melting during welding process was investigated by Katz and Rubinsky [46] employing an inverse finite element technique.

Considering that the heat transfer during the melting process is conduction-controlled, numerical solutions using finite difference methods were proposed by Petra [47], Pham [48,49], Menning and Ozisik [50], Charch and Khan [51] and Chen [52] to obtain results for this process. Likewise, a numerical approach for three-dimensional solidification was presented by Gilmore and Guceri [53]. Velocity maps for the melt vortical motion of pure gallium were illustrated by Webb and Viskanta [54] which are considered as an indication to the dramatic role of natural convection in the melting process. Under a quasi-steady assumption, natural convection -controlled heat transfer during melting of PCM in vertical rectangular enclosures heated from side was analysed by Yeung [55] using a conduction layer approximate method and taking inclination and curvature of the solid- liquid interface into account by dividing the interface into series of steps. $\cdot$ **424998**

Mushy zones which surround the solid-liquid interface during the melting process was investigated in a recent study in (1990) by Shyy and Chen [56] using a finite-element computational techniques. More distortion was exhibited in phase boundaries due to higher Ra numbers or lower Ste numbers. Convection strength was found to be increased for higher Ra numbers. Another recent study in (1990) was presented by Kim and Kaviany [57] in which coordinate transformation tech-

nique was employed in an immobilization finite-difference method for solution of melting problem without consideration of convection effects.

2.4 Analytical Works

Compared to numerical and experimental works, less number of analytical works about phase change problems are existed. Even in the available analytical works, natural convection was not considered at all in their developed solutions order to avoid mathematical complexity. Optimal linearization method was applied by Vujanovic [58] and perturbation theory was used by Aziz and Benzies [59] to study the conduction mode of heat transfer in such problems. Analytical study presented by Vujanovic and Baclic [60] in (1976) was based on Gauss's principle and Goodman studies (1964) to solve conduction- controlled melting of a semi-infinite solid. Weinbaum and Jiji [61] employed perturbation method to solve conduction heat transfer equations during melting process. Likewise, inverse Stefan conduction-controlled melting and solidification problem was solved by Rubinsky and Shitzer [62]. Characteristics of thermal and fluid flow was investigated by Ramachandran et al [63]. Heat transfer equations during solidification in a finite slab were solved by Soloman [64] for large Ste and Biot numbers, by Chan et al [65] for arbitrary initial liquid temperature and by Charach and Zoglin [66] using time-dependent perturbation theory. Solidification of Glauber salt ($T_m = 32°c$) was investigated by Gutman [67] and Mashema and Haji-Sheikh [68] using Galerkin finite-difference method. Even recent analytical works investigating melting and solidification processes dealt with these problems without any consideration to convection mode of heat transfer in the melt region, such as the study presented by Li and Barber [69] in (1989) who used perturbation method for the solution, and that of Lecomte and Batsale [70] who proposed an approximate solution of Neumann's problem in (1991).

Horizontal cross-section of the installation.

East-west vertical cross-section of the solar enclosure
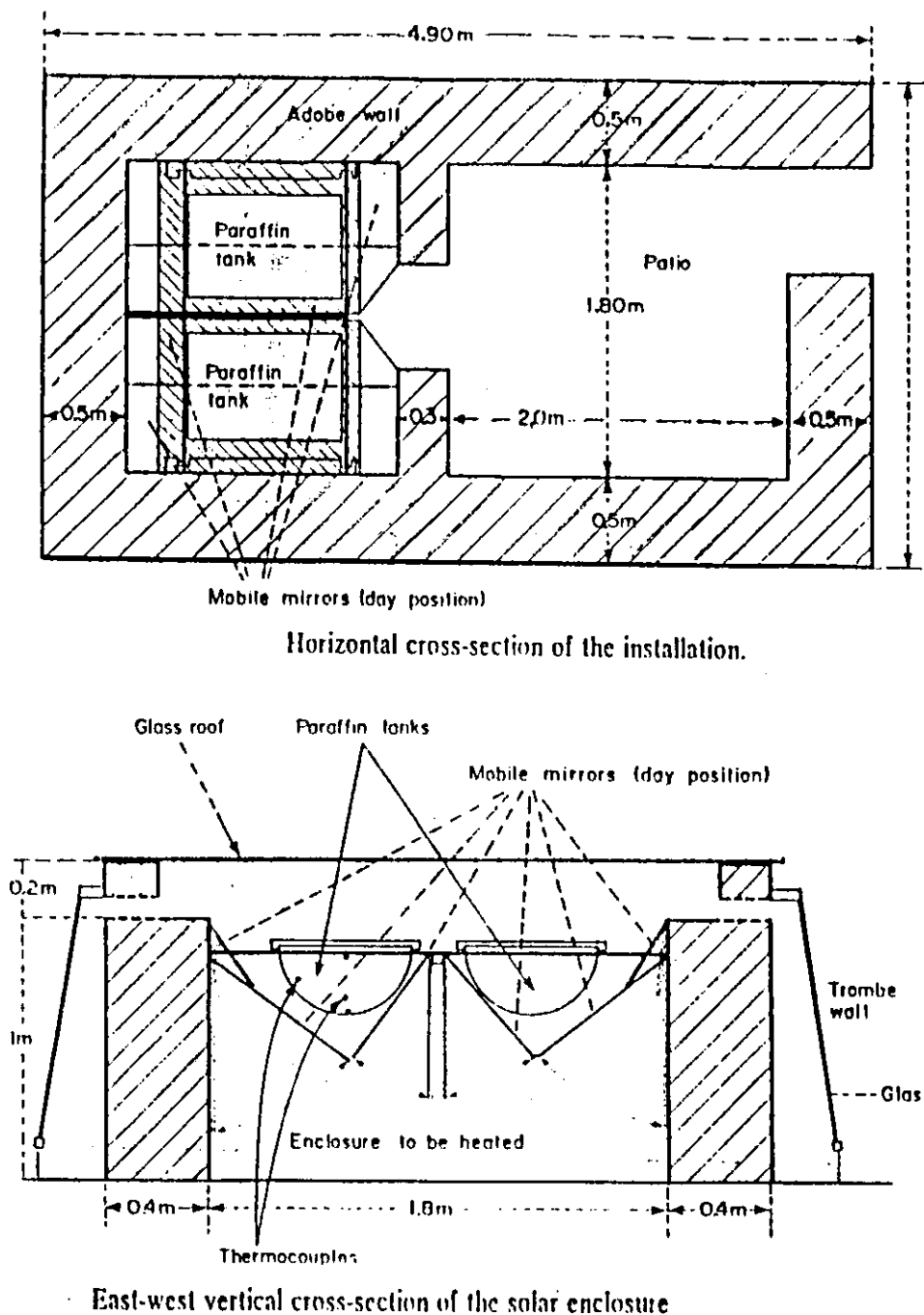
Fig.2.1 Tanks of paraffin wax $(T_m = 36°c)$ used as solar PCES collection system and employed to maintain the room temperature of an experimental chicken brooder within $22 - 30°c$ [5].

Flat plate exchanger input
(temperature regulated)

Double glazing
(system 2)

South face
surrounding
insulation

Flat plate
exchanger

0.2 m
Thick
insulation

Paraffin wall
(system 1)

Back room
(system 3)

Flat plate
exchanger
output

1.7m

Fig.2.2 PCES solar wall filled with paraffin wax $(T_m = 40/50°c)$ and used to run an air-conditioning system of an experimental back room [34].

$T_{2,xx}$

T_h

Auxiliary heater

MODELS 2&3

T_7

MODEL 3
UAHTX$_1$

Wax store with
heat exchanger

Collector

Fully mixed
preheat tank

MODEL 1

T_s

$T_{c(mons)}$

$T_{1,xx}$

Pump 1

Pump 2

T_6

Fig.2.3 TES system assisted by PCES sub-system consisting of hybrid water- paraffin wax $(T_m = 55°c)$ heat exchanger [10].

Chapter 3

THE EMPLOYED MODEL

3.1 Model Description

The employed physical model is shown schematically in Fig.3.1a, which shows a rectangular enclosure of height H, width B and depth D (less than H), whose all its walls are insulated except the left side vertical wall along which heat is supplied isothermally. The enclosure contains a pure Phase-Change Material (PCM) of such a type which can be used in Thermal Energy Storage (TES) systems in forms of latent heat of fusion storage. Typical PCMs are paraffin waxes, Glambers salt and gallium. In this study of the melting process, the PCM is initially in its solid state at an initial temperature, T_i, then heat is added to the enclosure through its vertical wall. The melting process starts when the temperature of the solid layer which is adjacent to the heated wall reaches its melting temperature, T_m. The solid-liquid interface propagates in the positive direction of x-coordinate.

Melting of the paraffin waxes enclosed in rectangular configurations were of fundamental interest in the previous works in this art, as discussed in chapter II. Accordingly, this model was selected to be employed in this work, also because this configuration is found in many residential, scientific and industrial applications. On the other hand, the paraffin waxes are selected as PCMs because they are low cost by-product of the petrochemical industry, of high heat of fusion, chemically stable in cycling [8] and has a range of melting temperatures near the ambient temperatures which reduces the heat losses into the surroundings [12].

Insulation for all
sides except the
left side.

Heating

Phase change material
enclosed inside rect-
angular enclosure

H

D

B

(a)

y

H

Liquid phase

Solid phase

Heating

(b)

Solid-liquid
interface

0   B   X
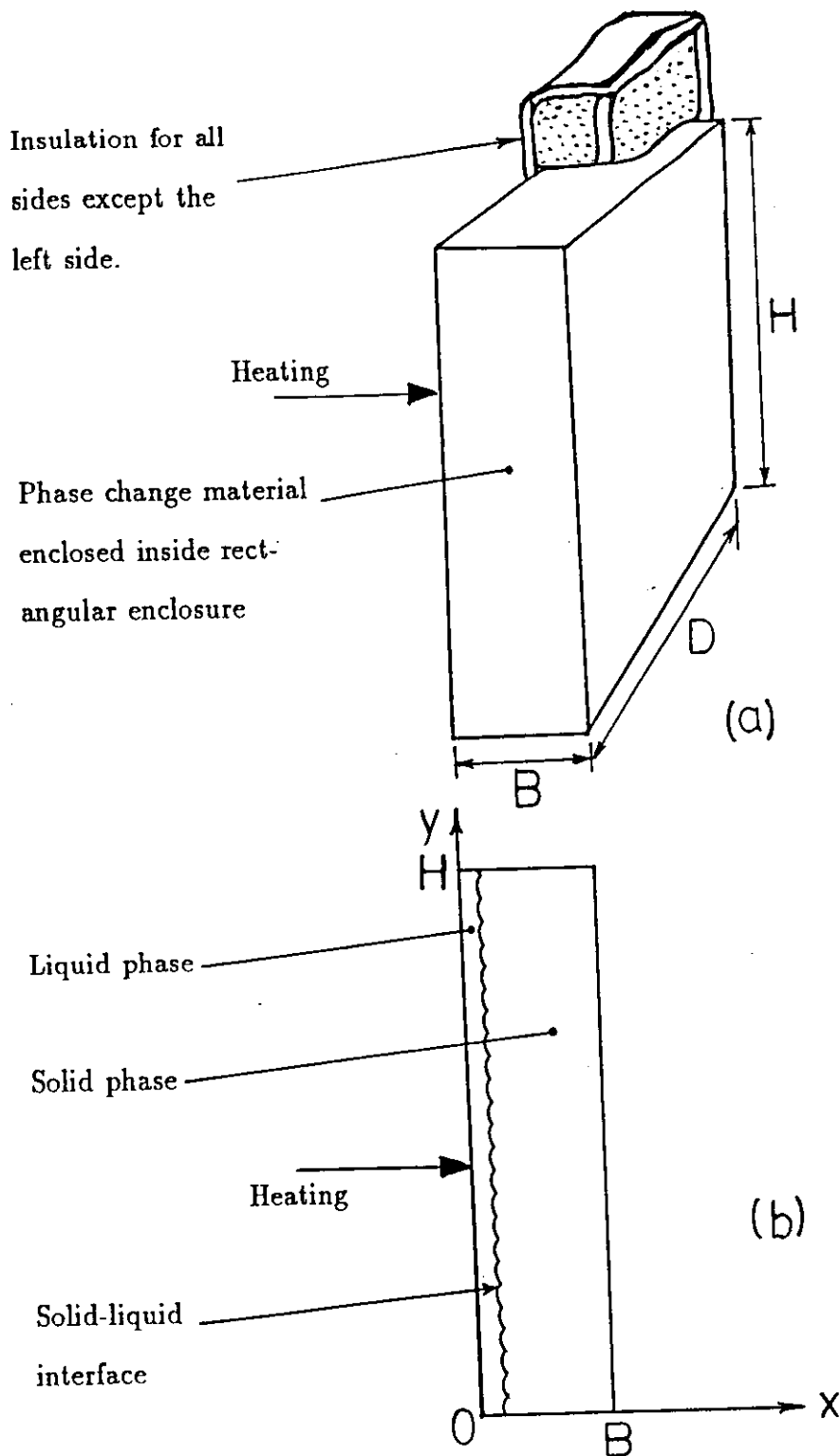
Fig.3.1 A scheme for the physical model (employed for this work) consisting of a rectangular enclosure containing PCM and subject to isothermal heating from side. (a) Oblique view (b) Elevation view representing an early stage of the melting process.

In addition to the advantages mentioned above, some of the paraffin waxes are desirable to be used as test materials in the laboratories because, in their liquid phase, they are transparent to the visible radiation, and this allows for photographic observations and optical measurements of displacement, position, inclination and shape of the solid-liquid interface, noting that the test enclosures, which contains paraffin waxes, are made of transparent plexiglass material. Finally, PCMs thermophysical properties are well established and thus facilitate the proper nondimensionalization which is necessary in generalizing the results. In this work, n-octadecane is mainly employed as the enclosed PCM. This type of paraffin waxes was studied or used as test material in many previous works of this art as discussed in details in chapter II. Thermophysical properties of notable PCMs are found in Appendix A.

3.2   Assumptions

In this section, some assumptions will be proposed so as to simplify the solution. On the other hand, these assumptions are used to be proposed in such class of problems knowing that their effects on the accuracy of the results are negligible. In the following are the assumptions on which this analytical study is built.

1. The heat losses through the insulated walls of the enclosure are negligible and are considered of zero value.

2. The effects of inertia terms are negligible compared to the buoyancy and viscosity effects.

3. Prandtl number of the employed material is larger than a unity (actually, Pr numbers of PCMs are much bigger than a unity).

4. The phase change material is isotropic and homogeneous in its solid and liquid phases and its liquid phase is Newtonian and incompressible.

5. The solid-liquid interface is smooth and plane.

6. The inclination angle of the interface is time-dependent only and independent on the altitude which means that the interface is straight (not curved).

7. As the temperatures range in this class of problems is small, thus, the variation

in the thermophysical properties of the PCM for each of its solid and liquid phases is negligible and these properties are assumed to be of constant values.

8. The motion of the liquid particles in the vertical (or longitudinal) direction is only within the two boundary layers.

3.3   Physical Analysis Of PCM Melting Process

The PCM enclosed in the employed model shown in Fig.3.1a is initially in its solid phase. As a result of heat addition, the temperature of the layer adjacent to the heated wall starts to increase. As the melting temperature, T_m is reached, melting of PCM starts and the solid-liquid interface (the melting front) moves in the positive direction of x-coordinate. The rate of melting depends essentially on thermophysical properties of PCM, such as its thermal diffusivity, conductivity, latent heat of fusion and specific heat. Fig.3.1b shows the interface in its vertical position at an early conduction-controlled heat transfer stage of melting process. Classically, conduction had been assumed to be the sole mode of heat transfer through the liquid phase during melting process. Recently, it was observed that the natural convection contribution is several times greater than that of conduction. It was found that the heat transfer in the liquid region during the melting process is controlled only by pure conduction for an early short period [9,15,17]. The transition from conduction regime into natural convection regime is represented in Fig.3.2. In general, the melting process consists of the following four stages [9]:

1. Start-up time.

2. Conduction regime.

3. Transition from conduction to natural convection.

4. Convection regime.

The start-up time is the period required for the temperature of the solid layer adjacent to the vertical heated wall to raise from, T_i, to T_m.

The second stage starts when melting starts, so, a small melt layer is built - up through which the heat is transferred by pure conduction due to temperature gradient from T_w at the heated wall to T_m at the solid liquid interface. Through this period, the interface is vertical and smooth. The time of the first and second stages are found to be a small fraction of the melting process[9]. Thus during the conduction regime there is a horizontal temperature gradient and vertical isotherms in the liquid phase. The temperature of the heated wall, T_w, and the temperature of the liquid phase, T_l, in the case of melting at constant rate of heating, increase with time during the second stage without being altitude-dependent.

As heating is continued, the melt layer thickness increases, and the third stage starts during which the transition from conduction mode to natural convection mode occurs. It was established that during this stage, the following four thermophysical phenomena build-up [9,54]:

1. Vertical thermal stratification of the liquid core.

2. Forming of two boundary layers.

3. Vorticity of liquid particles around the liquid core.

4. Start of the solid-liquid interface inclination.

At the end of the short conduction regime, hotter liquid particles move upwards and the colder ones move downwards due to the density variation. This causes a vertical thermal stratification in the liquid core, thus, there will be horizontal isotherms and vertical temperature gradient in the liquid core as shown in Fig.3.4. Meanwhile, two boundary layers build up, a hot one adjacent to the vertical heated wall, and a colder one adjacent to the inclined solid-liquid interface. The liquid particles close to the heated wall will be heated and accordingly will move upwards along this wall gaining heat all their way up until their temperature reach a maximum value, T_w, at the top level of the enclosure where they deflect away from the heated wall towards the solid-liquid interface, which is colder than these heated particles, so, the liquid particles flow downward along the interface loosing its gained heat to the interface all

their way down causing the solid surface to melt. The melting capability decreases to the minimum at the bottom of the enclosure where its temperature is equal to T_m. The motion of the heated particles in the vertical direction occurs only through the passage of the boundary layers while the liquid core is stationary. The motion of the liquid particles discussed above is a vortical type in clockwise direction as shown in Fig.3.5. The third stage is also a short one during which the temperature of the liquid core increases with time until it reaches a maximum value and thereafter does not change.

The fourth stage starts when the liquid core temperature begins its steady state period which follows the above third stage immediately and continues until the end of the melting process. During this fourth stage, the heat transferred is mainly controlled by the natural convection mode. The temperature distribution in the liquid core is in its final plateau where it depends only on the altitude and no longer is a function of time. The same situation is for the temperature distribution in the hot boundary layer. The melting rate of the top of the solid-liquid interface is faster than the lower parts, thus, photographic observations in many experimental works [9,12,13,35,56] shows the top of the interface as a convex surface. This is due to the maximum of the flow motion and temperature of the liquid particles at the top of the enclosure.
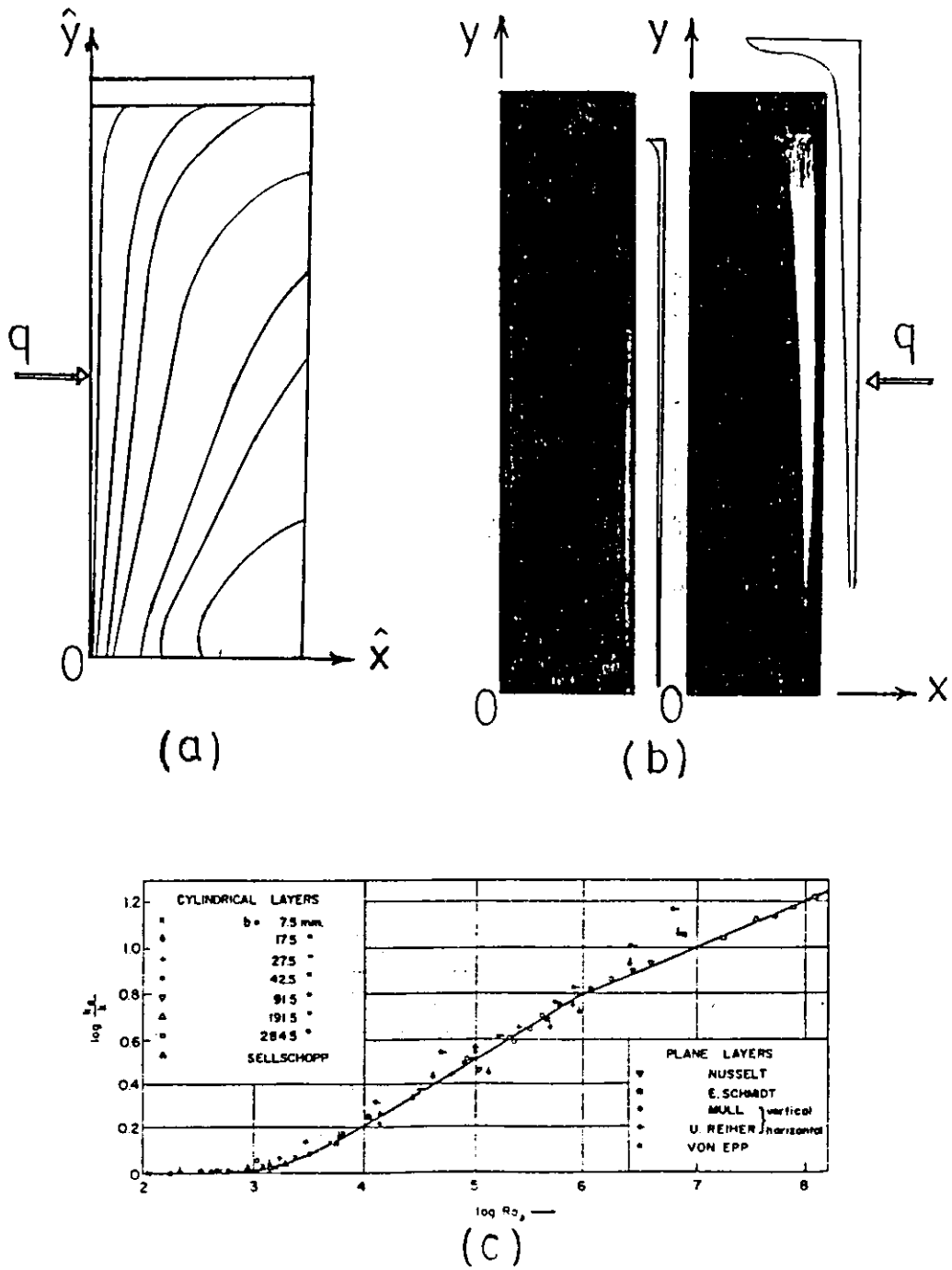
Fig.3.2 The transition from conduction regime into natural convection regime at the early stages of the melting process. (a) Experimental time evolution [15] (b) Photographs [9] (c) Graphical [22].
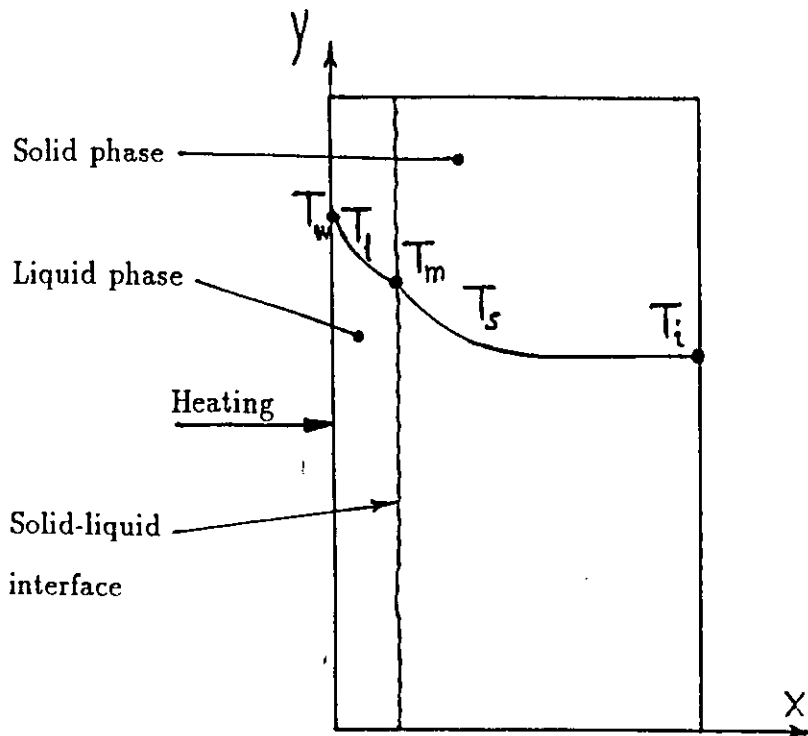
Fig.3.3 Temperature distribution during the conduction regime at early stages of the melting process.

(a)   (b)
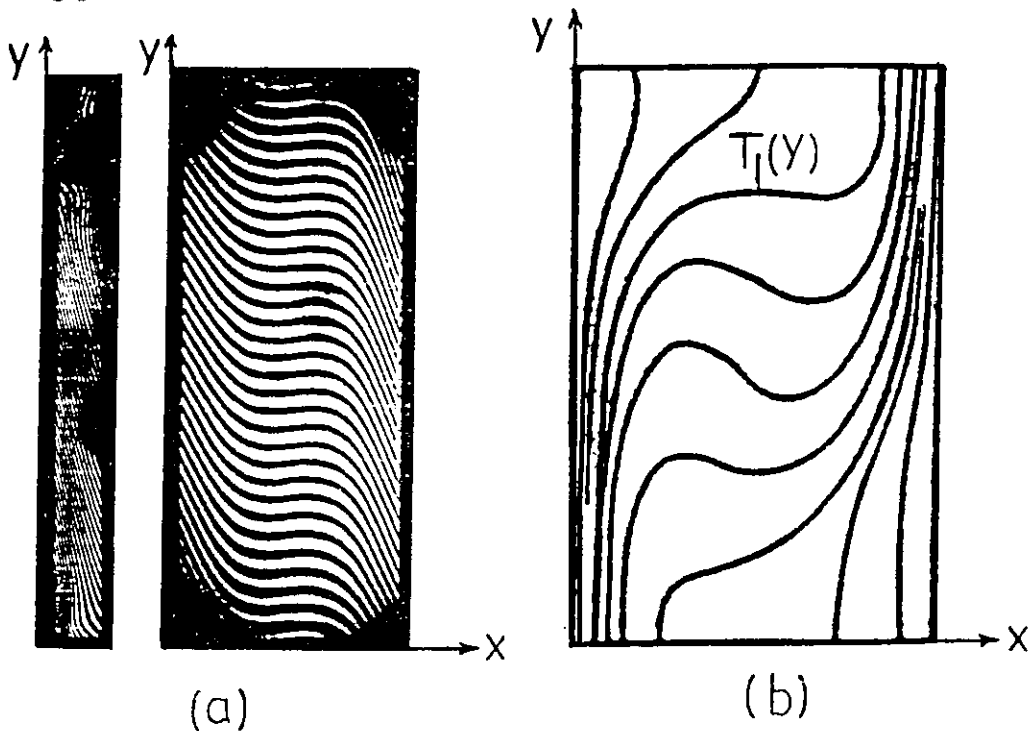
Fig.3.4 The thermal stratification and the horizontal isotherms during the convection stage of the melting process. (a) Interferograms (b) Computer solutions [22].
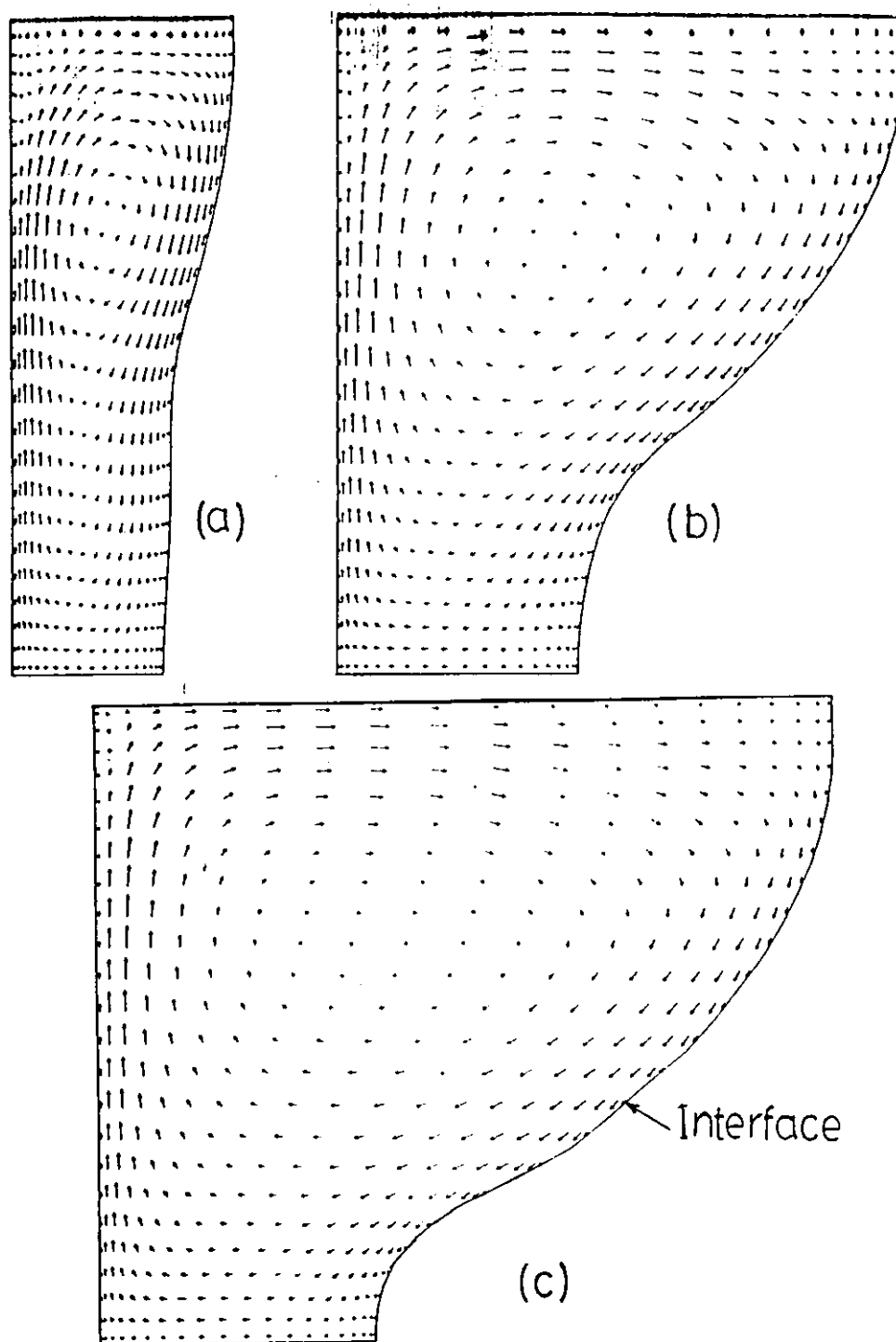
Fig.3.5 Time-evolution of the velocity field of the liquid particles vortical motion during the natural convection stage of the melting process, where (a), (b) and (c) are at early, middle and late times of that stage respectively [54].

3.4 Mathematical Analysis Of PCM Melting Process

Phase-change problems are inherently difficult and nonlinear due to the motion of the solid-liquid interface, thus, location of the interface is not known a priori and must be followed as a part of the solution. Even for the conduction mode in the liquid phase in these problems, exact analytic solution can be developed only for limited number of particular cases, and the most notable among them is known as Neumann's solution [20] for a semi-infinite one-dimensional slab initially at a uniform temperature. Therefore, recourse is made either to approximate analytical methods or to numerical methods. In addition, as natural convection has been considered, recently, as the predominant mode of heat transfer in the liquid phase during the melting process, more complexity and nonlinearity is added to these problems. Further, if the interface inclination is taken into account, the problem will be much more complicated.

In this work, natural convection regime is considered the sole mode of heat transfer in the liquid phase, and the corresponding solution concentrates on the fourth stage. The main governing equations for each boundary layer are the continuity, momentum and energy conservation equations. The hot boundary layer is attached to the main (x, y) coordinates system (as shown in Fig.4.1), while the cold boundary layer is attached to (x', y') coordinate system. The velocity and temperature profiles for both boundary layers are assumed in forms of simple quadratic expressions which agree very well with exact solutions of pure natural convection problems [9,22,71,72,73]. The governing equations will be integrated to obtain integral equations for both of the hot and cold boundary layers. Then the two integral equations will be refined, reduced and finally matched to each other by using mass conservation principle between the two layers. The temperature distribution in the liquid core will be evaluated using the developed integral equations. There will be several mathematical steps directed, all the way, towards reducing the number of unknowns until analytical solution is developed.

Chapter 4

DEVOLEPMENT OF ANALYTICAL SOLUTION

4.1 Introduction

In this chapter, analytical solution is developed for the melting process. Fig.4.1 shows a schematic elevation view of the employed rectangular model which contains a PCM of large value of latent heat of fusion. The equations developed in this work are in terms of dimensionless parameters and can be generalized to any PCM. N-octadecane is employed to facilitate the proper nondimensionalization. The hot boundary layer is adjacent to the vertical heated isothermal wall and attached to the main (x, y) coordinates system. The relatively cold boundary layer is adjacent to the solid-liquid interface and attached to (x', y') system of coordinates which is moved linearly while is being turned in clockwise direction with time led by the interface propagation. As an approximation, the interface is assumed smooth and straight despite its actual curved surface (especially at its top).

In the following sections there are individual investigations for the hot and the cold boundary layers, the liquid core, the solid-liquid interface and its time evolution, the solid phase, the mass conservation between the two layers, the melting rate, the heat storage rate, the effects of the different dimensionless numbers and the optimum size of the enclosure.
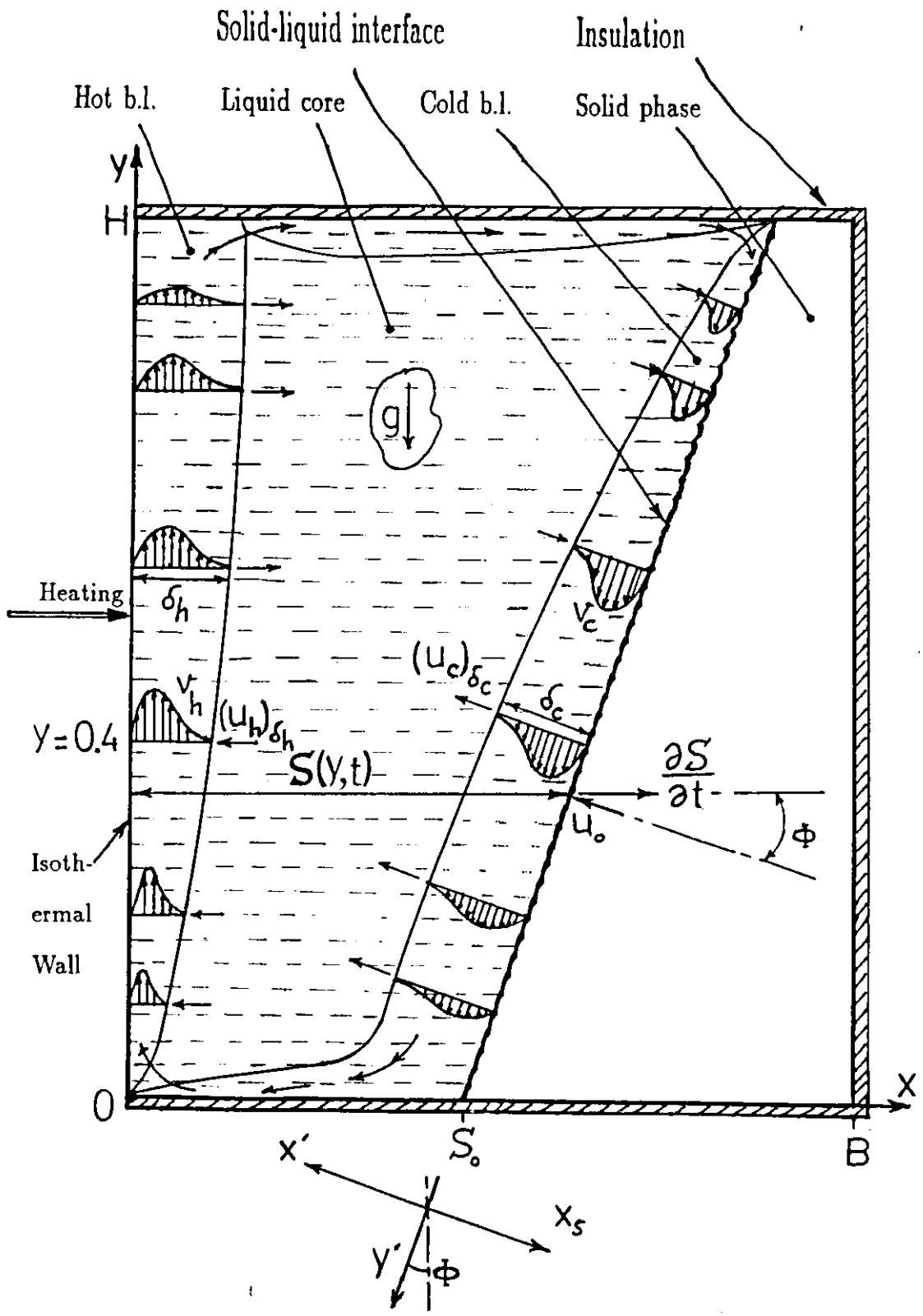
Fig.4.1 Schematical cross-sectional elevation of employed rectangular enclosure containing PCM and subject to isothermal heating from vertical side. The variations of velocity profile vs altitude, within the two boundary layers, are shown.
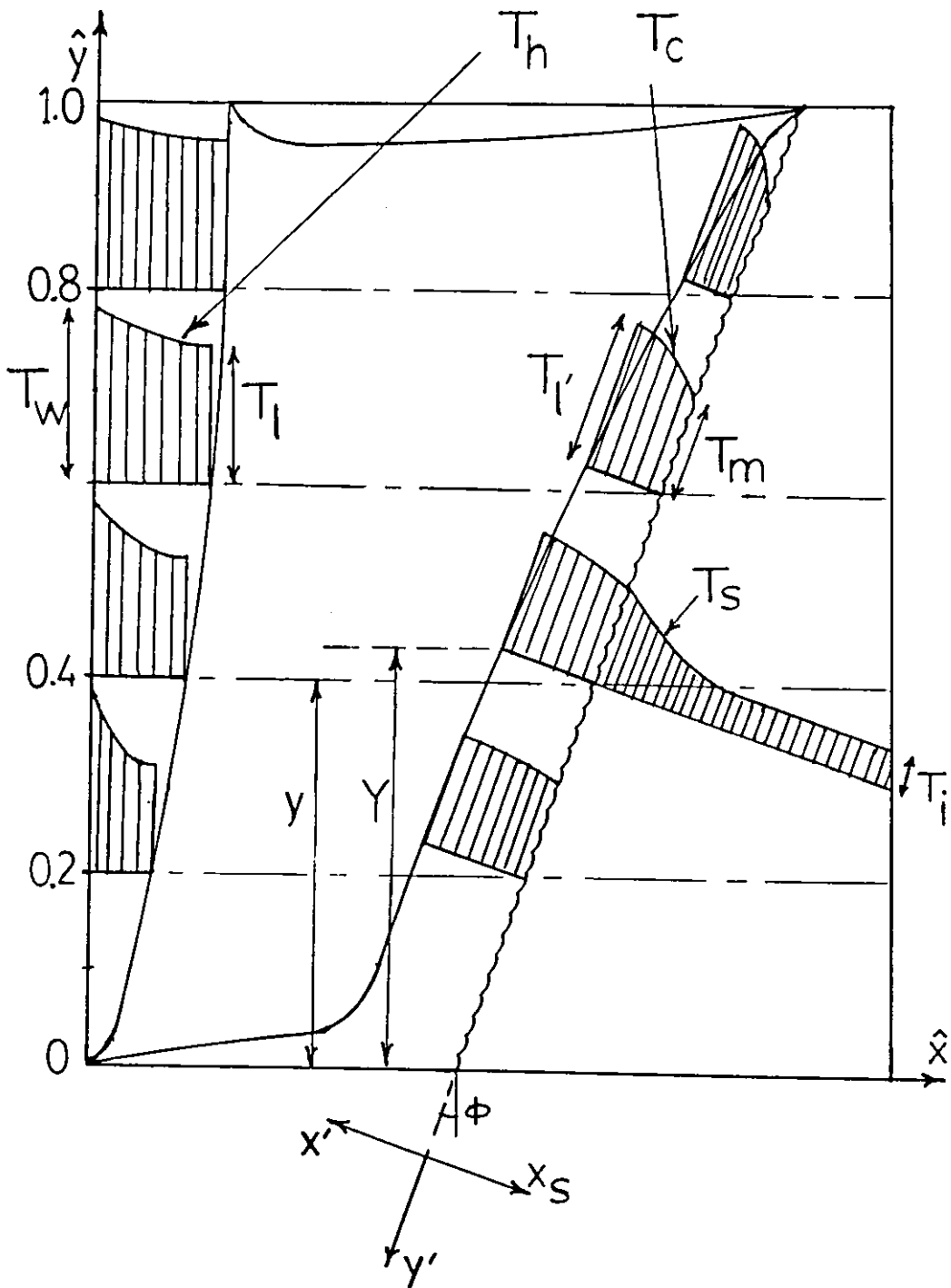
Fig.4.2 The employed rectangular enclosure model (as proposed in Fig.4.1). The variations of temperature profiles vs altitude, within the two boundary layers, are shown.

The variations in the velocity and temperature profiles, as shown in figures 4.1 and 4.2, indicate that the momentum energy ebbs when the thermal energy predominates and vise versa. As will be evaluated later on in the following sections in this chapter, the momentum energy is in its peak value at $\hat{y} \simeq 0.4$ for the hot boundary layer and at $\hat{y} \simeq 0.63$ for the cold boundary layer. On the other hand, the thermal energy is in its peak value at the top of the enclosure.

4.2 The Hot Boundary Layer

This boundary layer is adjacent to the heated isothermal wall. Its leading edge is at the bottom of the wall. Its governing equations are the continuity, momentum and energy conservation equations for $0 \leq x \leq \delta_h$ as follows [9,22,71,72,73]:

$$\frac{\partial v_h}{\partial y} + \frac{\partial u_h}{\partial x} = 0 \tag{4.1}$$

$$\frac{\partial(v_h^2)}{\partial y} + \frac{\partial(v_h u_h)}{\partial x} = g\beta(T_h - T_l) + \nu \frac{\partial^2 v_h}{\partial x^2} \tag{4.2}$$

$$\frac{\partial(v_h T_h)}{\partial y} + \frac{\partial(u_h T_h)}{\partial x} + \frac{\partial T_h}{\partial t} = \alpha_l \frac{\partial^2 T_h}{\partial x^2} \tag{4.3}$$

Assuming quadratic expressions [9,22,71,72,73] for the profiles of the velocity, v_h, and the temperature, T_h, for $0 \leq x \leq \delta_h$.

$$v_h = V_h \frac{x}{\delta_h}(1 - \frac{x}{\delta_h})^2 \tag{4.4}$$

$$T_h = T_l + \Delta_{wl}(1 - \frac{x}{\delta_h})^2 \tag{4.5}$$

From equation (4-4), it can be shown that $v_h = 0$ at $x = 0$ and δ_h, and that the maximum local value of v_h is at $x = \frac{\delta_h}{3}$, also, $\frac{\partial v_h}{\partial x} = 0$ at $x = \delta_h$. From equation (4-5), it is found that at $x = \delta_h$, $T_h = T_l$ and $\frac{\partial T_h}{\partial x} = 0$ and at $x = 0$, $T_h = T_w$. These results are displayed for the hot boundary layer in the velocity distributions as shown in Fig.4.1 and the temperature distributions as shown in Fig.4.2.

Integrating the continuity equation from 0 to $x = \delta_h$

$$\int_0^{\delta_h} \frac{\partial u_h}{\partial x} dx = -\int_0^{\delta_h} \frac{\partial v_h}{\partial y} dx \qquad (4.6)$$

Thus,

$$(u_h)_{\delta_h} = -\frac{\partial}{\partial y}(\frac{1}{12}V_h \delta_h) \qquad (4.7)$$

Equation (4-7) represents the lateral velocity of the liquid particles at the outer boundary, $(x = \delta_h)$. Integrating the momentum equation from 0 to $x = \delta_h$ and neglecting the inertia terms compared to the effects of the buoyancy and viscosity terms [8,18,19], the local characteristic velocity is

$$V_h = \frac{g\beta}{3\nu}(\triangle_{wl}\delta_h^2) \qquad (4.8)$$

Integrating the energy conservation equation from 0 to $x = \delta_h$, using Leibnitz rule and using equations (4-7) and (4-8), the integral equation of the hot boundary layer is

$$\frac{1}{3}(2\delta_h\frac{\partial T_l}{\partial t} + \triangle_{wl}\frac{\partial \delta_h}{\partial t}) + \frac{g\beta}{180\nu}(-\triangle_{wl}\delta_h^3\frac{\partial \triangle_{wl}}{\partial y} + 6\triangle_{wl}^2\delta_h^2\frac{\partial \delta_h}{\partial y}) = \frac{2\alpha_l\triangle_{wl}}{\delta_h} \qquad (4.9)$$

This is a time-dependent equation which governs the motion and temperature of the liquid within the hot boundary layer for a short conduction-to- convection transition period, after which, thermal stratification in the liquid core reaches its steady state which exists until the end of the melting process. The two transient terms in this equation vanish when the natural convection steady state starts. Thus, equation (4-9) yields to an altitude-dependent equation. Substituting the corresponding dimensionless variables, in this equation, it becomes

$$\frac{1}{360}[(-\hat{\delta}_h^4)\frac{\partial \hat{\triangle}_{wl}}{\partial \hat{y}} + 6\hat{\triangle}_{wl}\hat{\delta}_h^3\frac{\partial \hat{\delta}_h}{\partial \hat{y}}] = 1 \qquad (4.10)$$

4.3 The Cold Boundary Layer

The cold boundary layer is adjacent to the solid-liquid interface and is inclined, together with its attached (x',y') coordinates system, with the interface time-dependent inclination. The temperature and velocities distribution inside this

layer is a function of altitude and time during the whole melting process. The governing equations for the cold boundary layer are the continuity, momentum and energy conservation equations as follows [9,22,71,72,73]

$$\frac{\partial v_c}{\partial y'} + \frac{\partial u_c}{\partial x'} = 0 \tag{4.11}$$

$$\frac{\partial (v_c^2)'}{\partial y'} + \frac{\partial (v_c u_c)}{\partial x'} = -(g\cos\phi)\beta(T_c - T_{l'}) + \nu\frac{\partial^2 v_c}{\partial x'^2} \tag{4.12}$$

$$\frac{\partial (v_c T_c)}{\partial y'} + \frac{\partial (u_c T_c)}{\partial x'} + \frac{\partial T_c}{\partial t} = \alpha_l\frac{\partial^2 T_c}{\partial x'^2} \tag{4.13}$$

The velocity and temperature profiles are assumed in quadratic forms for $0 \leq x' \leq \delta_c$ as

$$v_c = V_c\frac{x'}{\delta_c}(1 - \frac{x'}{\delta_c})^2 \tag{4.14}$$

$$T_c = T_{l'} - \triangle_{l'm}(1 - \frac{x'}{\delta_c})^2 \tag{4.15}$$

Where δ_c is the local thickness of the cold boundary layer along the inclined x'-direction which makes a time-dependent inclination angle $\phi(t)$ with the main x-direction. V_c is the local characteristic velocity for the cold boundary layer.

Similar to that of the velocity and temperature distributions of the hot boundary layer, the same analysis is done for the cold boundary layer, thus, from equation (4-14), it is found that $v_c = 0$ at $x' = 0$ and δ_c, and that the maximum local value of v_c is at $x' = \frac{\delta_c}{3}$ measured in x'-coordinate direction, also, $\frac{\partial v_c}{\partial x'} = 0$ at $x' = \delta_c$. From equation (4-15), it is found that at $x' = \delta_c$, $T_c = T_l'$ and $\frac{\partial T_c}{\partial x'} = 0$ and at $x' = 0$, $T_c = T_m$. These results are displayed for the cold boundary layer in the velocity distributions as shown in Fig.4.1 and the temperature distributions as shown in Fig.4.2.

The temperature distribution, $T_{l'}$, of the liquid core along the inclined outer boundary of this layer is always slightly higher than the corresponding horizontal isotherm level of the liquid core, T_l, and this difference increases as the interface inclination increases. Thus, another altitude coordinate, Y, is attached to $T_{l'}$ as shown in Fig.4.2. Integrating the continuity equation from 0 to $x' = \delta_c$, it yields to

$$(u_c)_{\delta_c} - (u_c)_0 = -\frac{\partial}{\partial y'}(\frac{1}{12}V_c\delta_c) \qquad (4.16)$$

Where $(u_c)_{\delta_c}$ and $(u_c)_0$ are the local lateral velocities of the liquid particles in x'-direction at $x' = \delta_c$ and 0 respectively. Integrating the momentum equation from 0 to $x' = \delta_c$ and neglecting the inertia terms compared to the effects of buoyancy and viscosity terms [9,18,19], the local characteristic velocity is

$$V_c = (cos\phi)\frac{g\beta}{3\nu}(\triangle_{r_m}\delta_c^2) \qquad (4.17)$$

Integrating the energy conservation equation from 0 to $x' = \delta_c$, using equations (4-16) and (4-17), substituting the corresponding dimensionless variables and $(-y/cos\phi)$ instead of y' in the developed integral equation, the cold boundary layer dimensionless integral equation is

$$\frac{1}{3}[2\hat{\delta}_c\frac{\partial\hat{\triangle}_{r_m}}{\partial\tau} - \hat{\triangle}_{r_m}\frac{\partial\hat{\delta}_c}{\partial\tau}] + \frac{(cos\phi)^2}{180}[6\hat{\triangle}_{r_m}^2\hat{\delta}_c^2\frac{\partial\hat{\delta}_c}{\partial\hat{y}} - \hat{\triangle}_{r_m}\hat{\delta}_c^3\frac{\partial\hat{\triangle}_{r_m}}{\partial\hat{y}}] + \hat{\triangle}_{r_m}(\hat{u}_c)_0 + \frac{2\hat{\triangle}_{r_m}}{\hat{\delta}_c} = o$$
$$(4.18)$$

4.4   The Solid-Liquid Interface

After early stages are over and the transition stage is completed, the steady state takes place in controlling the heat transfer of the melting process and the heat supply is transferred into the cold boundary layer and the solid-liquid interface, thus, the solid layer is melted and the temperature of this melted layer is raised from T_m, through the temperature distribution of the cold boundary layer into a higher temperature T_i adding more hot thermally stratified liquid to the liquid core. The mathematical formulation of the above statements can be presented by applying heat balance for the whole system at the interface as expressed in the following equation

$$-\int_0^H k_l \frac{\partial T_h}{\partial x}|_{x=0}dy = \int_0^{H'}\int_0^{\delta_c} \rho_l c_l \frac{\partial T_c}{\partial t}dx'\,dy' + \int_0^{H'} k_l \frac{\partial T_c}{\partial x'}|_{x'=0}dy' \qquad (4.19)$$

After straightforward integration and doing the proper substitution, the result is the following solid-liquid interface energy balance dimensionless equation

$$\frac{1}{3}[2\hat{\delta_c}\frac{\partial\hat{\triangle}_{rm}}{\partial\tau} - \hat{\triangle}_{rm}\frac{\partial\hat{\delta_c}}{\partial\tau}] = \frac{2\hat{\triangle}_{wl}cos\phi}{\hat{\delta_h}} - \frac{2\hat{\triangle}_{rm}}{\hat{\delta_c}} \qquad (4.20)$$

Using equations (4-18) and (4-20), all time-dependent terms are eliminated, thus, the cold boundary layer general equation is reduced to

$$\frac{(cos\phi)^2}{180}[6\hat{\triangle}_{rm}^2\hat{\delta_c^2}\frac{\partial\hat{\delta_c}}{\partial\hat{y}} - \hat{\triangle}_{rm}\hat{\delta_c^3}\frac{\partial\hat{\triangle}_{rm}}{\partial\hat{y}}] + \hat{\triangle}_{rm}(\hat{u_c})_0 + \frac{2\hat{\triangle}_{wl}(cos\phi)}{\hat{\delta_h}} = 0 \qquad (4.21)$$

4.5 Mass Conservation Between The Two Boundary Layers

The vorticity motion of the liquid particles, which is shown in Fig.4.3, means that these particles pass out through the outer boundary of the cold layer at certain velocity travelling laterally through the liquid core, thereafter, entering into the hot layer through its outer boundary at the same velocity. A typical particle bath is shown in Fig.4.3. The horizontal entrainment velocities of the two boundaries represent the same horizontal liquid core if

$$\int_0^H (u_h)_{\delta_h} dy = \int_0^{H'} [(u_c)_{\delta_c} - (u_c)_0]dy' \qquad (4.22)$$

Substituting equations (4-7) and (4-16) in this equation and arranging the results in dimensionless terms, the entrainment relationship which matches between the boundary layers is mathematically formulated as

$$\hat{\triangle}_{wl}\hat{\delta_h^3} = (cos\phi)^2\hat{\triangle}_{rm}\hat{\delta_c^3} \qquad (4.23)$$

Equation (4-23) is a balance equation between the two buondary layers concerning all their corresponding parameters like the temperature, the velocity, the layer thickness and the inclination of the interface.
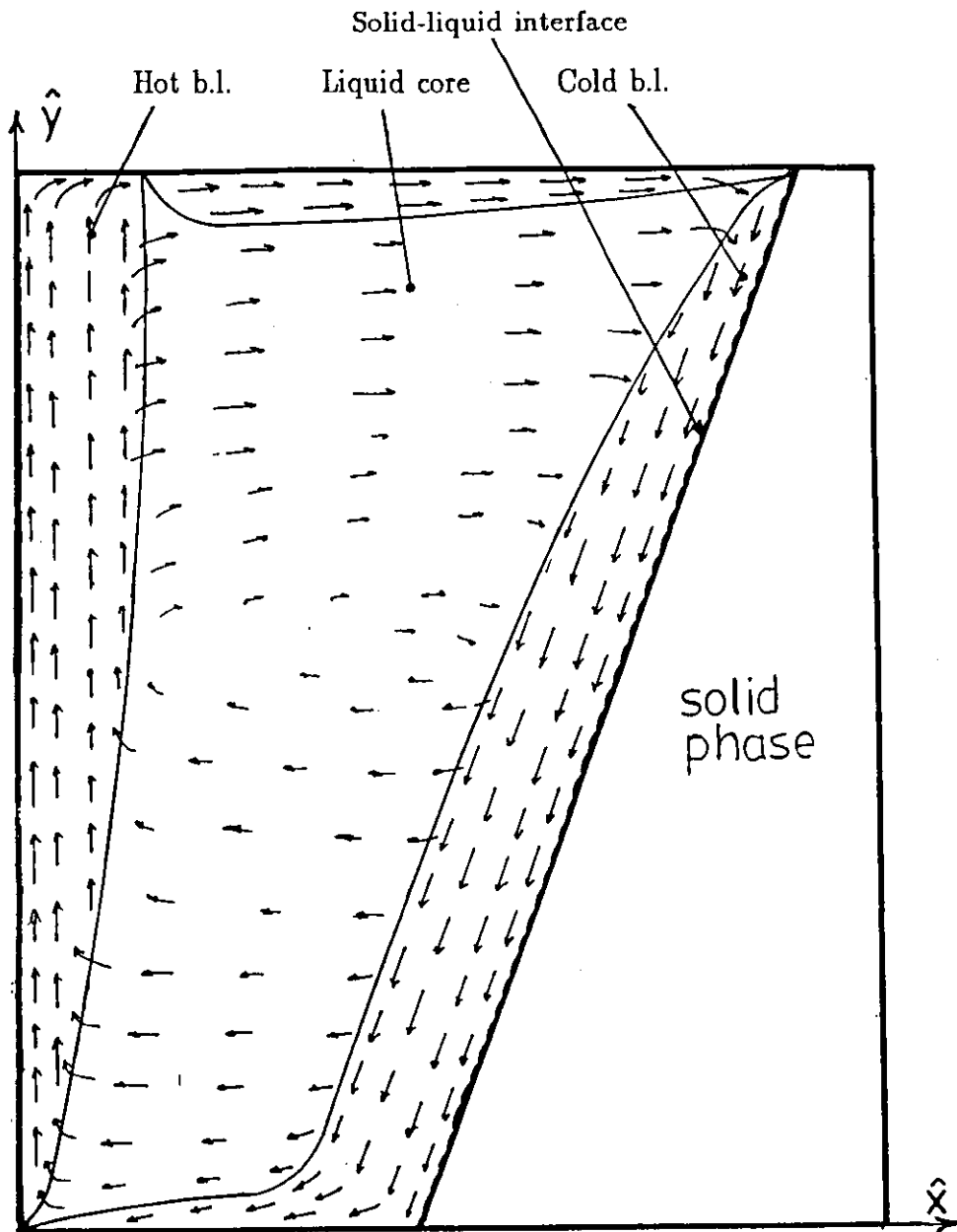
Fig.4.3 Typical particle paths for the liquid vorticity motion during melting process of a PCM in a rectangular enclosure heated from side vertical wall [59].

4.6 Evaluation Of Vertical Temperature Gradient In The Liquid Core

In this section, terms for $\hat{\triangle}_{wl}$ and $\hat{\triangle}_{fm}$ are evaluated. From the last section, it can be stated that the leading edge of the hot boundary layer is at the bottom of the vertical heated wall and that of the cold one is at the top of the solid-liquid interface. The temperature difference, $\hat{\triangle}_{fm}$, is of its maximum value at the top of the enclosure and is of zero value at the bottom, while $\hat{\triangle}_{wl}$ is maximum at the bottom and zero at the top. These statements show that $\hat{\triangle}_{wl}$ is proportional to $(1 - \hat{y})$, thus, using equation (4-10), it can be found that

$$\frac{\partial \hat{\triangle}_{wl}}{\partial \hat{y}}\Big|_{\hat{y}=0} = -\infty, \qquad \frac{\partial \hat{\delta}_h}{\partial \hat{y}}\Big|_{\hat{y}=0} = \infty \qquad (4.24)$$

The above analysis indicates that the liquid core temperature gradient and the hot boundary layer profile may be expressed as

$$\hat{\triangle}_{wl} = \hat{\triangle}_{wm}(1 - \hat{y}^n) \qquad (4.25)$$

$$\hat{\delta}_h = (\hat{\delta}_h)_{max}\hat{y}^m \qquad (4.26)$$

In order to evaluate the values of the proposed symbols, n and m, equations (4-10), (4-25) and (4-26) are used and found to be satisfied with values of $n = 3/2$ and $m = 1/4$. Thus, equations (4-25) and (4-26) yield to

$$\hat{\triangle}_{wl} = \hat{\triangle}_{wm}(1 - \hat{y}^{3/2}) \qquad (4.27)$$

$$\hat{\delta}_h = 2[\frac{15\hat{y}}{\hat{\triangle}_{wm}}]^{1/4} \qquad (4.28)$$

Temperature difference, $\hat{\triangle}_{fm}$, which is related to the inclined interface, is a function of its attached $\hat{Y}$-altitude which is given by

$$\hat{Y} = \hat{y} + \frac{\hat{\delta}_c \sin\phi}{Ra^{1/5}} \qquad (4.29)$$

Noting that $\hat{\delta}_c$ may be found from equation (4-23) as

$$\hat{\delta}_c = \hat{\delta}_h[\frac{\hat{\triangle}_{wl}}{\hat{\triangle}_{fm}(cos\phi)^2}]^{1/3} \qquad (4.30)$$

As the temperature difference between the heated wall and the solid-liquid interface is constant, then, using equation (4-27) it can be shown that

$$\hat{\triangle}_{lm} = \hat{\triangle}_{wm}\hat{y}^{3/2} \tag{4.31}$$

$$\hat{\triangle}_{\Gamma m} = \hat{\triangle}_{wm}\hat{Y}^{3/2} \tag{4.32}$$

Mathematical analysis is done for equations (4-30) and (4-32) and it is found that for values of $\hat{y} > 0.15$, the difference between $\hat{y}^{3/2}$ and $\hat{Y}^{3/2}$ is negligible. Accordingly, $\triangle_{\Gamma m}$ can be expressed as

$$\hat{\triangle}_{\Gamma m} = \hat{\triangle}_{wm}\hat{y}^{3/2} \tag{4.33}$$

Thus, the vertical temperature gradient in the liquid core is represented in equations (4-27) and (4-33), and the boundary layers profiles are represented in equations (4-28) and (4-30).

4.7 Variations Of The Velocity And Temperature Profiles, Within The Two Boundary Layers, VS The Altitude

Using equations (4-4), (4-8), (4-14), (4-17), (4-27), (4-28), (4-30) and (4-33), it is found that: $v_h \propto \hat{y}^{1/2}(1 - \hat{y}^{3/2})$ and $v_c \propto \hat{y}(1 - \hat{y}^{3/2})^{2/3}$. From these two proportionality relationships, the variations of the velocity profiles within the hot and cold boundary layers vs the altitude are evaluated and displayed in Fig.4.1. Also, it is found that the liquid upwards velocity, v_h, within the hot boundary layer, and the downwards one, v_c, within the cold boundary layer reach their peak values at $\hat{y} = 0.397$ and $\hat{y} = 0.627$ respectively, and both of them are of zero values at the bottom and the top of the enclosure.

On the other hand, the variation of the temperature profiles can be found from equations (4-5) and (4-27) for the hot boundary layer, and from equations (4-15) and (4-33) for the cold boundary layer. This is displayed in Fig.4.2.

4.8 Evaluation Of Solid-Liquid Interface Propagation

Both of the local thickness of the melting layer, $S(y,t)$, and its rate, $\frac{\partial S(y,t)}{\partial t}$, are functions of time and altitude. The heat flux which arrives into the solid-liquid interface is consumed in two parts:

- Melting rate of the solid phase at the interface.
- Raising the temperature of the rest of the solid phase.

This can be expressed in the following energy balance equation at the interface

$$\int_0^H Q_{sl}\rho_s \frac{\partial S}{\partial t} dy = \int_0^{H'} k_l \frac{\partial T_c}{\partial x'}\big|_{x'=0} dy' - \int_0^{H'} k_s \frac{\partial T_s}{\partial x_s}\big|_{x_s=0} dy' \qquad (4.34)$$

The temperature distribution in the solid phase can be approximated in a quadratic expression [18] as

$$T_s = T_i + \triangle_{mi}(1 - \frac{x_s}{\delta_s})^2 \qquad (4.35)$$

Where δ_s is the local thickness of an assumed thermal boundary layer in the solid phase. A simplified energy conservation equation of this layer can be expressed in a form analogous to the corresponding equation of the liquid phase, except that the vertical velocity component,v, should be omitted from the equation as

$$\alpha_s \frac{\partial^2 T_s}{\partial x_s^2} = \frac{\partial T_s}{\partial t} - (\frac{\partial S}{\partial t})(\frac{\partial T_s}{\partial x_s}) \qquad (4.36)$$

Where: $\qquad T_s\big|_{x_s=0} = T_m, \qquad T_s\big|_{x_s=\delta_s} = T_i$

Integrating this equation from 0 to $x_s = \delta_s$, it is found that

$$\delta_s = \sqrt{18\alpha_s t}, \qquad \frac{\partial T_s}{\partial x_s}\big|_{x_s=0} = -\frac{2\triangle_{mi}}{\delta_s} \qquad (4.37)$$

Substituting $(-dy/cos\phi)$ instead of dy' in equation (4-34), Using equations (4-15), (4-23), (4-27), (4-28), (4-30), (4-33) and (4-37) to accomplish the integration of equation (4-34) and using the corresponding dimensionless parameters, equation (4-34) yields to

$$\frac{Ra^{1/5}\rho_r}{Ste}\int_0^1 \frac{\partial \hat{S}}{\partial r} d\hat{y} = \frac{4}{25cos\phi}[2\hat{\triangle}_{wm}^{5/4}(cos\phi)^{2/3} - 3\frac{k_r \hat{\triangle}_{mi}}{\sqrt{\alpha_r \tau}}] \qquad (4.38)$$

This equation is the integral equation for the melting propagation along the whole solid-liquid interface. The term, $\frac{\partial S}{\partial \tau}$, is a function of three variables, $\tau, \hat{y}$ and ϕ. The inclination angle, ϕ, is a function of time only and it is independent on the altitude, y, due to the assumption that the solid-liquid interface is straight and smooth. The last right hand side term represents the initial condition of the solid PCM, which would be omitted if the initial temperature is equal to T_m. This case was used extensively in treatments of phase change problems [7,13,14,15,55,62]. Equation (4-38) should be refined. This is achieved in the following section.

4.9 Evaluation Of Time-Dependent Inclination Of The Solid-Liquid Interface

With reference to Fig.4.1, geometrically, we can find the relationship between the local melted layer thickness, $S(y,t)$, and the corresponding melted layer thickness at the bottom of the enclosure, $S_0(t)$, noting that, S is a function of time and altitude while S_0 is a function of time only. This relationship is

$$S = S_0 + y(tan\phi) \tag{4.39}$$

The rate of S_0 increment with time is much slower than that of the top of the interface where the activity of the natural convection mode is at its maximum rates while this activity is almost negligible at the bottom of the liquid core. This was observed and established in several previous experimental works [9,12,15,35]. Actually this is the main reason for the interface inclination.

In this work, it is stated that the slow melting rate at the bottom of the enclosure is due to the greater contribution of the conduction mode in the heat transfer process at the bottom of the liquid core. Accordingly, it is assumed, in this work, that the melted layer thickness at the bottom of the enclosure, S_0, is controlled by conduction mode of heat transfer and can be evaluated by employing the corresponding mathematical technique. In order to find the temperature gradient at the lowest edge of the interface, and accordingly to evaluate the rate of heat flux at this edge (which controls the rate of S_0 increment), the following exact solution of the partial

differential equation of the conductive heat transfer in terms of a temperature profile is proposed [20,22].

$$T_{cond.} = T_w - \triangle_{wm}[erf\frac{x}{2\sqrt{\alpha_l t}}]/erf(\lambda)$$ (4.40)

Where, 'erf' is the error function with its values are being tabulated in tables in most of text books. The value of the constant λ depends on the thermophysical properties of the test PCM, the initial conditions and the Stefan number. The melted layer thickness at the bottom of the enclosure, S_0, is dependent on the value of λ as in the following expression [20,22]

$$S_0 = 2\lambda\sqrt{\alpha_l t}$$ (4.41)

In dimensionless terms

$$\hat{S}_0 = 2\lambda\sqrt{\tau}$$ (4.42)

Applying the energy balance at the bottom of the liquid core in accordance with the assumed conduction mode control at the bottom, it is found that

$$-k_l\frac{\partial}{\partial x}(T_{cond.})|_{x=0} = Q_{sl}\rho_l\frac{dS_0}{dt} + (-k_l)\frac{\partial T_s}{\partial x_s}|_{x_s=0}$$ (4.43)

Using equations (4-34), (4-38) and (4-43), equation (4-43) yields

$$\frac{e^{-\lambda^2}}{\sqrt{\pi}erf(\lambda)} = \frac{\rho\lambda}{Ste} + \frac{2k_r\triangle_{mi}}{\sqrt{18\alpha_r}\triangle_{wm}}$$ (4.44)

Having evaluated the root of this equation, λ, then, S_0 can be found. In this work, it is found that for limited values of Stefan numbers, the following correlation can be proposed for the case when $\triangle_{mi} = 0$ and $Ste < 0.25$

$$\lambda = (\frac{Ste}{\rho_r\sqrt{\pi}})^{0.53}$$ (4.45)

This correlation reduces the time required for the trial and error steps which should be applied on equation (4-44) in order to find the value of λ. On the other hand, in TES systems, Stefan numbers are almost less than o.25 which means that this correlation almost suits these systems. Even in other ranges of Stefan numbers and in cases when $\triangle_{mi} \neq 0$, this correlation can be useful for the first guess of the value

of λ.

Differentiating equation (4-39), it yields

$$\frac{\partial \hat{S}}{\partial \tau} = \frac{d\hat{S}_0}{d\tau} + \frac{\hat{y}}{(cos\phi)^2}\frac{d\hat{\phi}}{d\tau} \qquad (4.46)$$

Substituting this equation in equation (4-38) and performing the corresponding integration, gives

$$\frac{d\hat{\phi}}{d\tau} = 2(cos\phi)^2(\frac{4(Ste)}{25(Ra)^{1/5}\rho_r(cos\phi)}[2(Ra)^{1/4}(cos\phi)^{2/3} - \frac{3k_r\hat{\triangle}_{mi}}{\sqrt{\alpha_r\tau}}] - \frac{\lambda}{\sqrt{\tau}}) \qquad (4.47)$$

This equation is the developed resultant equation of all the previous mathematical steps. The nonlinearity and complexity of the governing and the integral equations are being reduced till this equation has been obtained. But, it is still a nonlinear one and it is not possible to integrate it in its present form. On the other hand, experimental works show that the increment of ϕ can be approximated in a linear relation with time [11,14,15]. Thus, it can be assumed that $\hat{\phi} = f\tau$ for $\tau > \tau_0$, noting that the value of $\hat{\phi}$ is zero for the period of $0 < \tau < \tau_0$. The initial dimensionless time, τ_0, represents the period during which the conduction-controlled early stages of melting occurs while the solid-liquid interface is in its vertical position. When τ_0 is over, the natural convection mode starts to control the heat transfer in the liquid core. The value of the proportional constant, f, depends on Stefan and Rayleigh numbers, the thermophysical properties of the PCM and the initial conditions. If the assumed expression, $\hat{\phi} = f\tau$, is substituted in equation (4-47), the corresponding integration can be performed and the value of the constant f may be obtained through a trial and error procedure.

Actually, it is easier to use equation (4-47) in its present form and plot the obtained values of ϕ against time. Accurate results can be obtained even with time steps as large as 3600 seconds. The value of the conduction mode period, (τ_0), is determined by substituting zero value for ϕ in equation (4-47).

4.10 Time-Evolution Of The Melted Fraction

The evolution of the melted fraction, F, depends on the aspect ratio of the employed enclosure in addition to the interface inclination angle and time. The

calculations required to find the melted fraction should be distinguished into two stages:

1. Melted fraction 'before' the top of the interface becomes in contact with the rear wall of the enclosure.

2. Melted fraction 'after' this contact.

The two stages are shown schematically in Fig.4.4 which shows the importance of the aspect ratio especially at the later stages of the melting process. The inclination angle for the position when the interface top contacts the top corner of the enclosure which is the point p(B,H), is specified by ϕ_B with

$$H(tan\phi_B) = B - (S_0)_B \qquad (4.48)$$

Where $(S_0)_B$ is the melt thickness at the bottom of the enclosure when the interface inclination angle is ϕ_B. Determination of angle ϕ_B is an essential step and can be done during the plotting process of ϕ against the time. For values the inclination angle larger than the value of ϕ_B, the height of top of the solid phase is denoted by y_a which is given by

$$y_a = (B - S_0)/(tan\phi) \qquad (4.49)$$

The two following equations represent the melted fraction during the two corresponding stages, and both of them will be used later on in the numerical applications:

- 'Before' the contact of the solid-liquid interface with the point p(B,H), for $0 < \phi \leq \phi_B$:

$$F_b = \frac{1}{HB}[S_0 H + 0.5H^2 tan\phi] = A[\frac{\hat{S}_0}{(Ra)^{1/5}} + 0.5tan\phi] \qquad (4.50)$$

- 'After' the contact of the interface with point p(B,H), for $\phi_B < \phi < \pi/2$:

$$F_a = \frac{1}{HB}[HB - 0.5y_a(B - S_0)] = 1 - \frac{[1 - A\hat{S}_0/(Ra)^{1/5}]^2}{2A(tan\phi)} \qquad (4.51)$$

Where the subscripts b and a refer to 'before' and 'after' the contact respectivelly.

4.11 The heating Rate

During a short start-up period, the temperature of the enclosed PCM is raised from T_i into a temperature profile $T_s(x_s, t)$ according to equation (4-35). From this equation, we find that $T_s(x = 0) = T_m$ at the end of the start-up period. During the conduction-controlled melting stage, which immediately follows the start-up period, the liquid core temperature is raised according to equation (4-40), then at the end of this stage and through a short transition stage, the liquid core is thermally stratified in a vertical temperature gradient. It was found that these three early stages of the melting process are short and would not exceed 30 minutes [9,15,44]. Thus, in this work, the heating rate during the last stage only will be studied, which is the natural convection-controlled stage, as it starts when the thermal stratification is completed and continues till the end of the melting process.

Using equations (4-5), (4-27), (4-28), (4-30), and (4-33), the average heat flux, coefficient of heat transfer and Nusselt number for both of the vertical heated wall of the enclosure and the solid-liquid interface are found in the following expressions:

- At the heated vertical wall of the enclosure:

$$(\hat{q}_w)_{av} = 0.453(Ra)^{1/4} \tag{4.52}$$

$$(\hat{h}_w)_{av} = 0.68(Ra)^{1/4} \tag{4.53}$$

$$(Nu_w)_{av} = 0.30(Ra)^{1/4} \tag{4.54}$$

- At the solid-liquid interface:

$$(\hat{q}_m)_{av} = 0.34(Ra)^{1/4}(cos\phi)^{2/3} \tag{4.55}$$

$$(\hat{h}_m)_{av} = 0.63(Ra)^{1/4}(cos\phi)^{2/3} \tag{4.56}$$

$$(Nu_m)_{av} = 0.22(Ra)^{1/4}(cos\phi)^{2/3} \tag{4.57}$$

Noting that:

$$q_w = h_w \triangle_{wl} \tag{4.58}$$

$$\hat{q}_w = \hat{h}_w \hat{\triangle}_{wl}/(Ra)^{1/5} \tag{4.59}$$
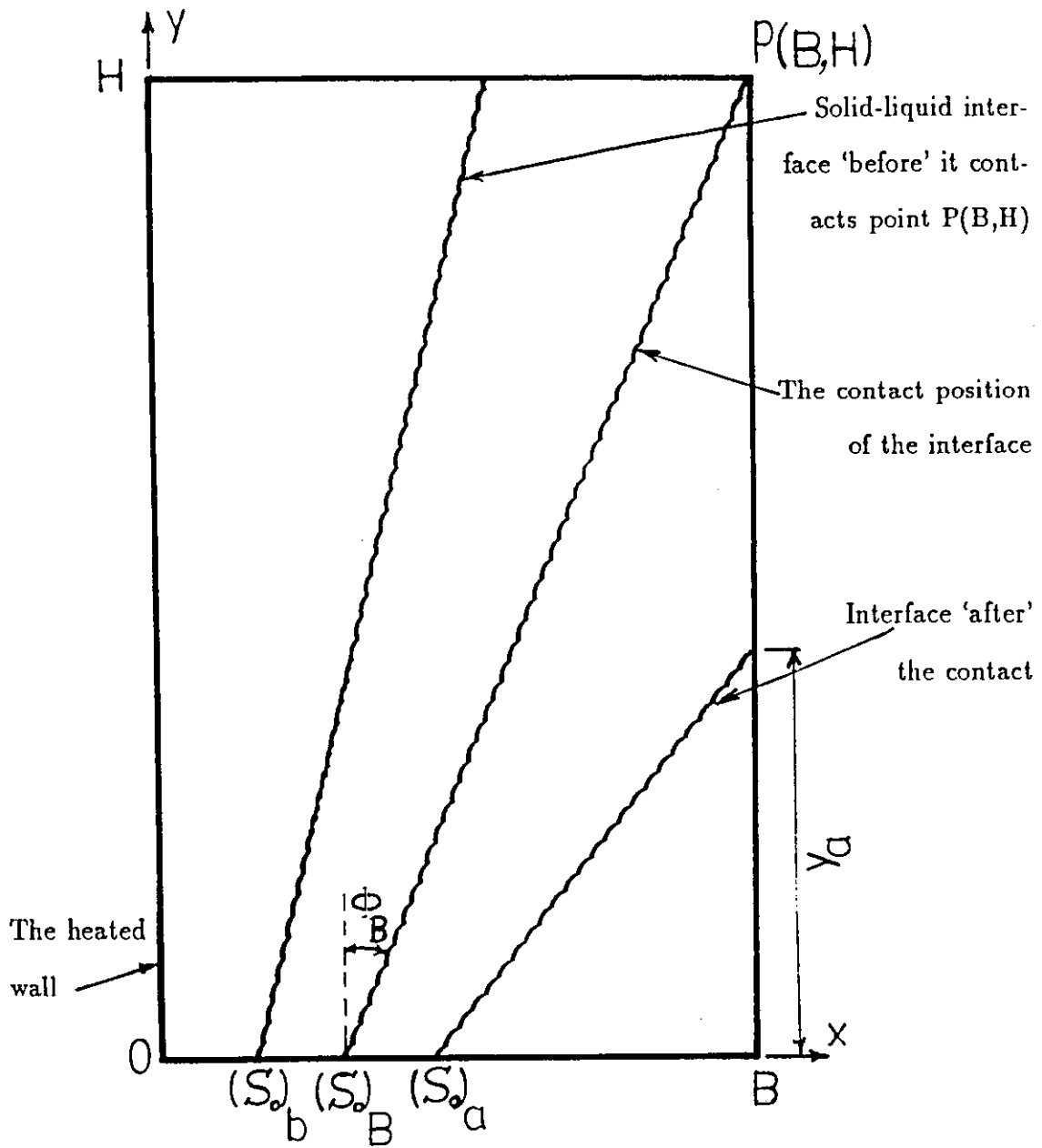
Fig.4.4 .The two stages of the melted fraction evolution: before the solid- liquid interface contacts the top of the enclosure, which is point p(B,H), and after this contact.

Chapter 5

RESULTS

5.1 Introduction

In this chapter, the results of the time evolution of the solid-liquid interface and its inclination angle, the melted fraction, the average Nusselt number and the average heat supply will be evaluated and compared against both experimental and theoretical results of selected previous works so as to demonstrate the efficiency and accuracy of the analytical solution of this work.

5.2 Time-Evolution Of The Solid-Liquid Interface And Its Inclination Angle

In this section, the results of the time evolution of the position, shape and inclination of the solid-liquid interface obtained using the developed analytical solution of this work will be compared against the same data obtained experimentally and numerically by selected previous works.

Comparisons will be done against previous works [7,15,35] which had employed rectangular transparent epexiglass experimental cells filled with n-octadecane paraffin wax as a suitable transparent test PCM, and used photographic observations to follow and distinguish the shape, position and inclination of the solid-liquid interface during the melting process of this PCM.

Experimental results obtained by Benard et al [15] are displayed in Fig.5.1 representing the position and shape of the interface at certain times until the end of the melting process, for a duration of about 12 hours, thus, this experimental work

is considered a typical one for comparison with this work and it is proposed as

the first example for this purpose. The employed rectangular is of relatively larger values of height and aspect ratio compared to other similar works. The corresponding experimental matrix is substituted in the developed analytical equations of this work, which they are equations (4-41), (4-44), (4-45) and (4-47). Then, results are obtained, for the same times used in the experimental work, and displayed in the figure representing the position and inclination of the solid-liquid interface. As shown in the figure, the agreement with the experimental results is well as the inclination and position of the interface obtained in this work are close to those obtained experimentally and the Solid-Liquid Interface propagation with time in both works is almost the same. As shown in the figure, the dashed lines are almost parallel to the solid lines except at the top of the interfaces. However, for higher values of y and over certain limited period of time during the melting process, the experimental results show that the top of the interface becomes curved while the results of this work show that it is a straight surface. This deviation is due to the assumption that the inclination angle of the interface, ϕ, is independent on the altitude, y. Further, the interface propagation is faster in this work than that in the experimental one. This is due to the actual heat loss across the sides of the experimental cell while this loss is assumed to be negligible in this analytical work.

Experimental results obtained by Okada [35] are displayed in Fig.5.2 as solid lines representing the interface position and shape at certain times of melting process. The employed rectangular is of small height and aspect ratio. The duration of the test in this experimental work is about 2 hours and much shorter than that in the first example. The interface is of a convex-concave shape, due to the small height and aspect ratio of the enclosure, and its curvature at its top is opposite to that in the first example. Substituting the corresponding experimental matrix in the equations of this analytical work, results are obtained for the same times and plotted in the same figure as dashed lines representing the interface position and inclination. As shown in the figure, the agreement between this work and the experimental one is well. The melting propagation obtained in this work is faster than that of the

experimental one in the lower half of the enclosure and it is slower in the upper

half of the enclosure which is a different case than that in the first example. This statement indicates that the faster propagation compensates the slower one and the result is a melting rate close to that of the experimental work.

Experimental results proposed for a third experimental example were obtained by Viskanta et al [7] as shown in Fig.5.3 as solid lines representing the shape and position of the interface at certain times of melting process. The experimental matrix is substituted in the equations of this work, then results are obtained and plotted in the figure which shows that the agreement with the experimental one is well. The deviation between the two works are for the same reasons as discussed in the first example.

The fourth comparison example is with numerical study results obtained by Yeung [55] which are displayed in Fig.5.4 as solid lines representing the shape and position of the solid-liquid interface at certain times of the melting process. The employed model is similar to that in the first example. The informations matrix is substituted in the developed equations of this work, then results are obtained and plotted in the figure which shows that the agreement with the numerical study results is well and better than that in the cases of the experimental examples concerning the solid-liquid interface propagation rate and the curvature of the top of the interface. With reference to figures 5.1 and 5.4, in general, the numerical study results can be considered as average between the experimental results and the results of this work. On the other hand, the values of the propagation rate of the interface bottom, S_0, obtained in this work can be considered as average between the experimental and the numerical study results as shown in the same two figures.

The numerical study results obtained by Gadgil et al [44] are plotted in Fig.5.5. The employed model is a rectangular enclosure containing n- octadecane paraffin wax and is relatively of large values of aspect ratio and Stefan number, thus, the melting propagation was faster and the melting period was shorter than those in the previous examples. The corresponding numerical matrix is substituted in the developed equations of this work. Results are evaluated and displayed in the figure

which shows that the agreement of the results of this work with the numerical ones is well and better than that in the cases of the experimental examples.
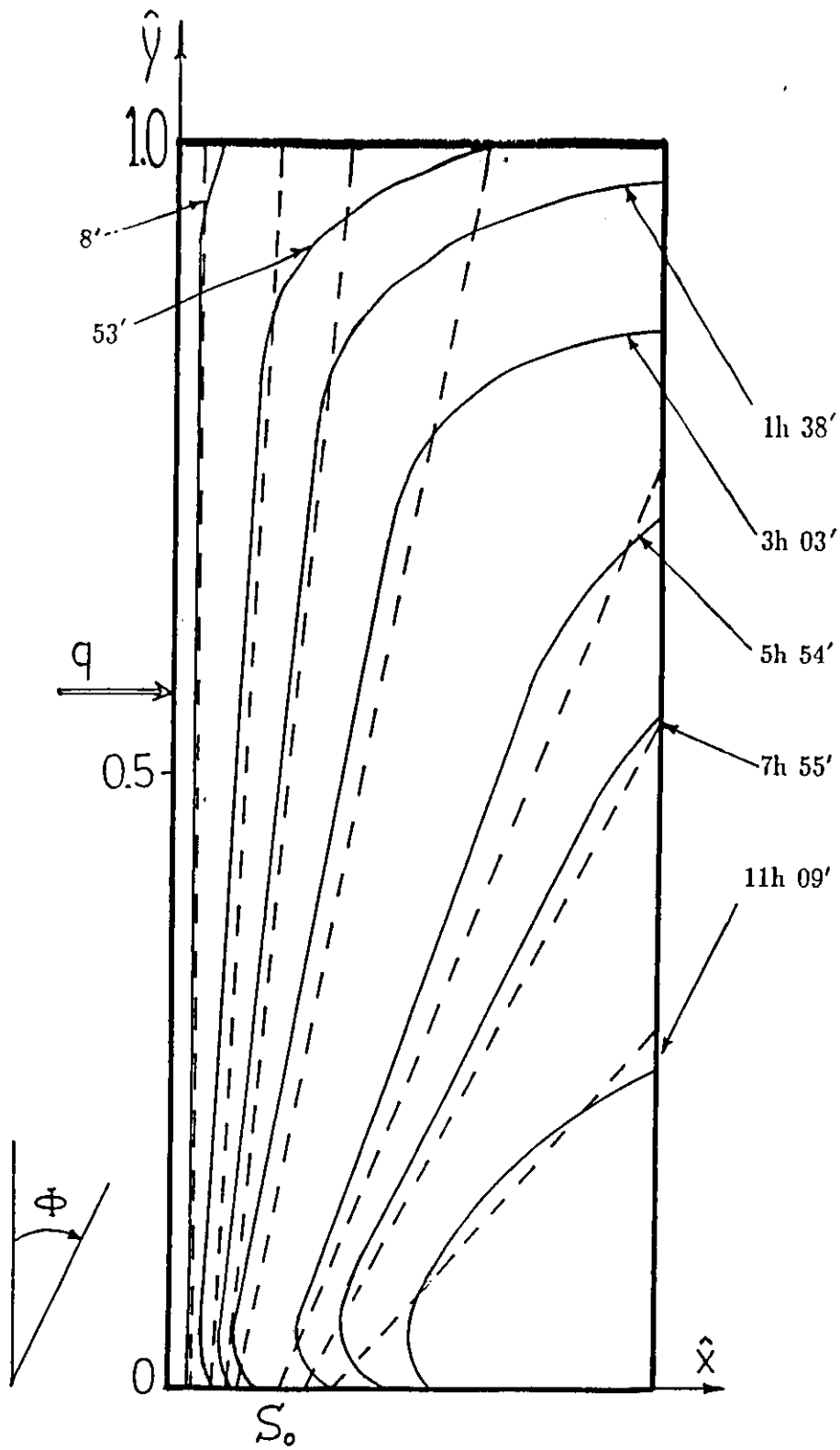
Ra	Ste	$\triangle_{wm}$	T_m	H	W	A	Pr
10^9	0.084	$9°c$	$28°c$	0.175m	0.069m	2.54	54

Fig.5.1 Time evolution of the solid-liquid interface and its inclination angle, (ϕ).

(—-) experimental results of [15]. (- - -) results of this work.
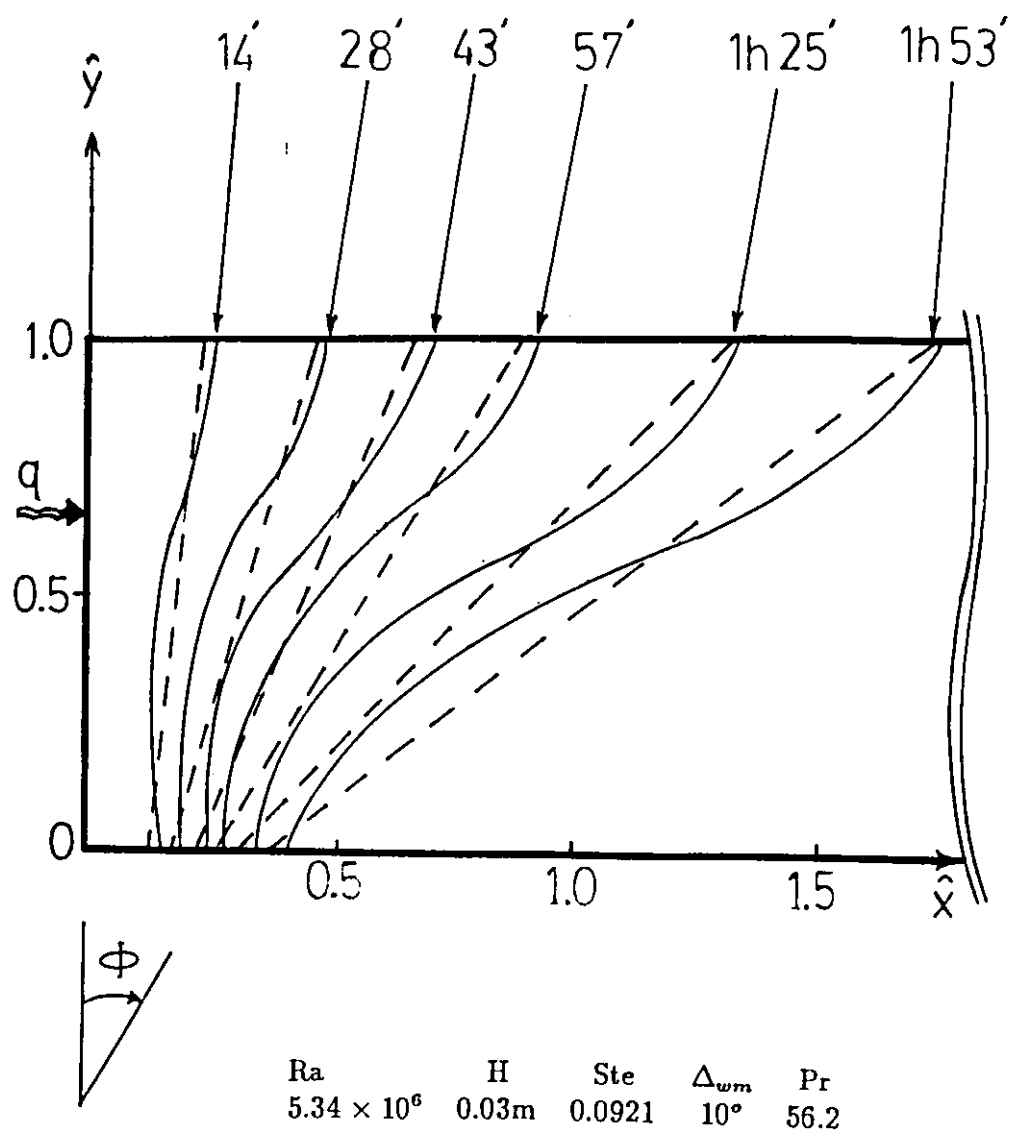
Fig.5.2 Time evolution of the solid-liquid interface and its inclination angle. (——) experimental results of [35]. (- - -) results of this work.
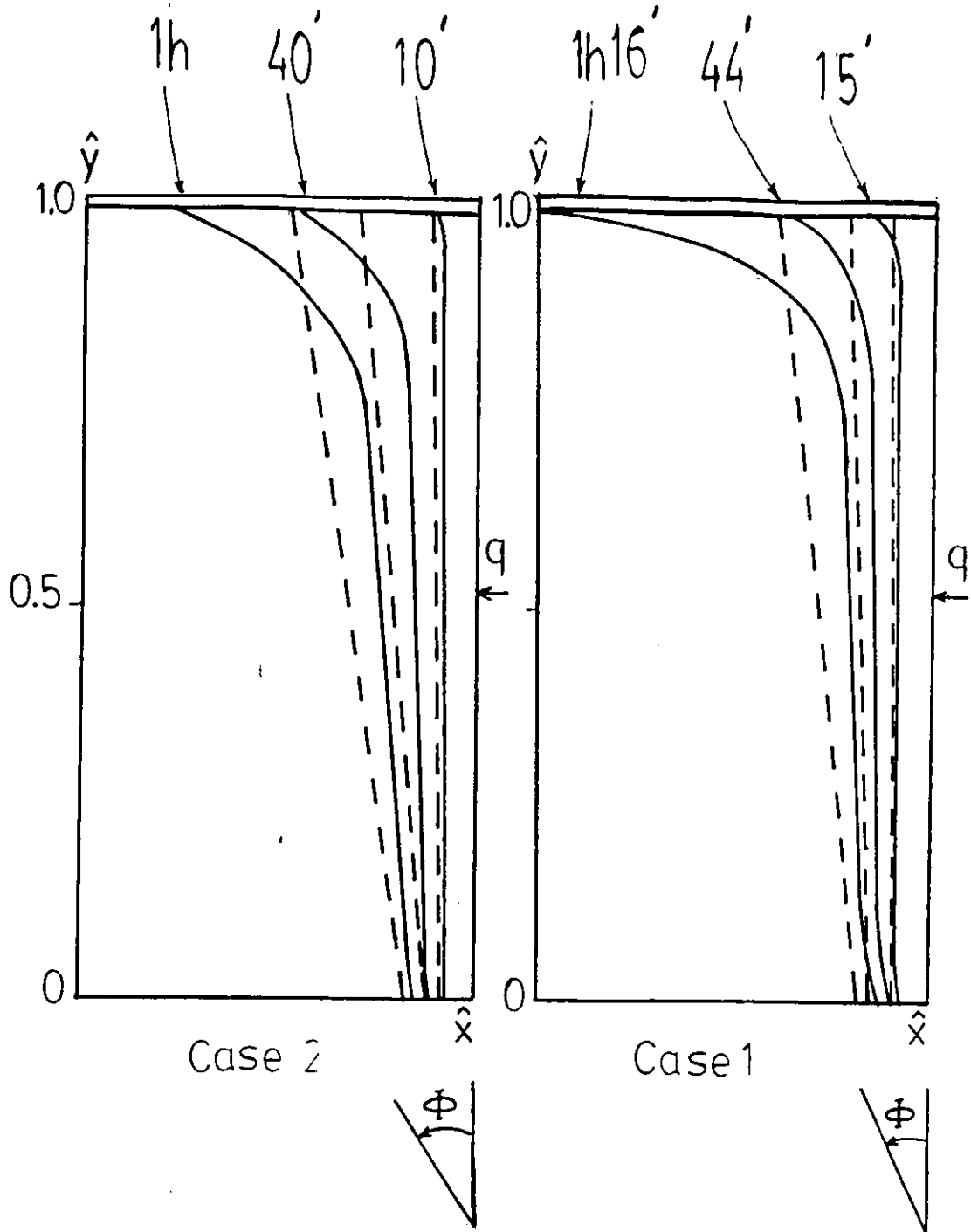
	H	T_m	A	Pr	Ra	Ste	Δ_{mi}	Δ_{wm}
Case 1	0.078m	28°c	2	54	10^8	0.09	0°c	10°c
Case 2	0.078m	28°c	2	54	1.4×10^8	0.132	20°c	14.5°c

Fig.5.3 Time evolution of the-liquid interface and the inclination angle. (- - -) this work. (—) experimental work [7].
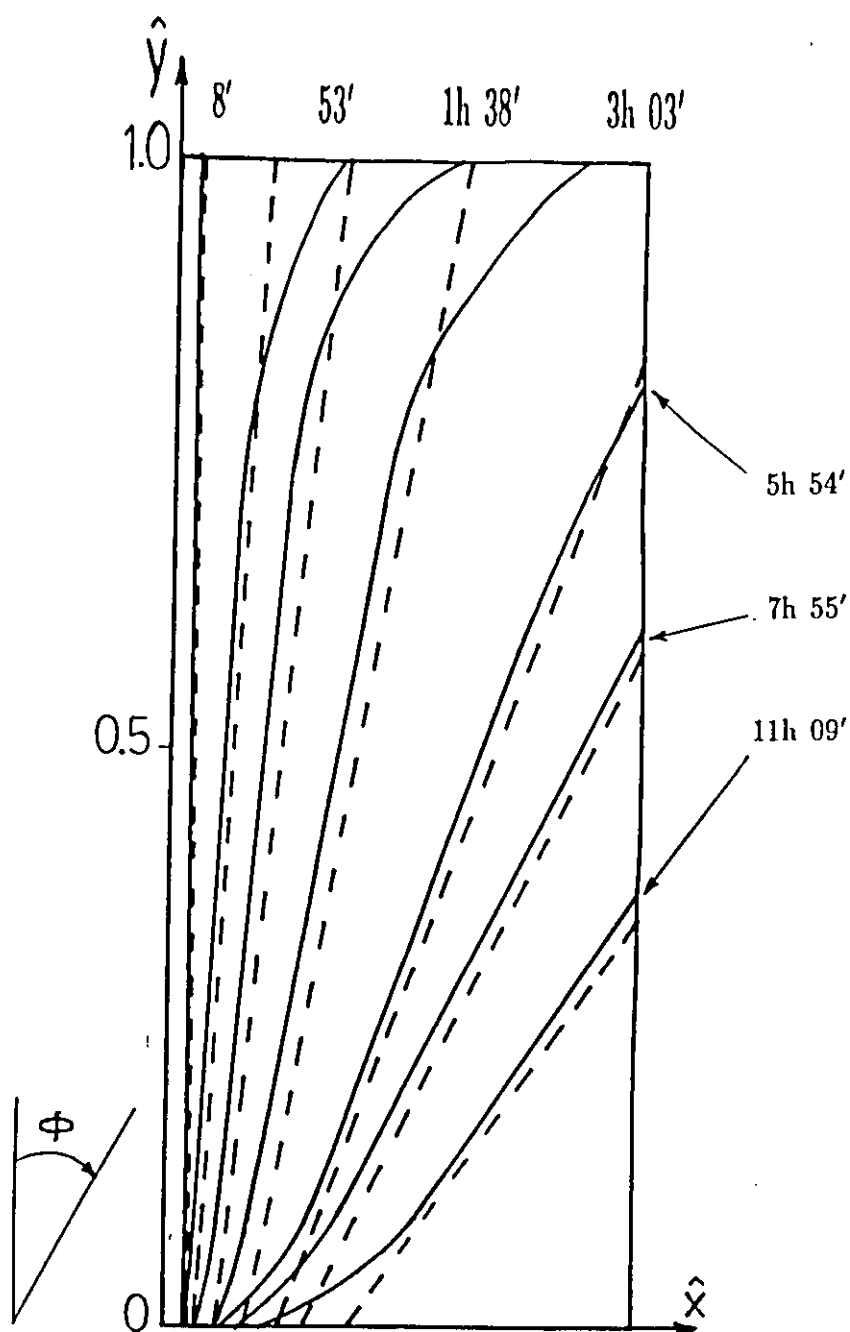
Ra	Ste	$\triangle_{wm}$	T_m	H	W	A	Pr
10^9	0.084	$9°c$	$28°c$	$0.175m$	$0.069m$	2.54	54

Fig.5.4 Time evolution of the solid-liquid interface and its inclination angle. Numerical study results of [55] (——). Results of this work(- - -).

$H = o.13$

$A = 5.25$

$Ra = 10^9$

$Pr = 55$

$\Delta_{mi} = 0^\circ c$
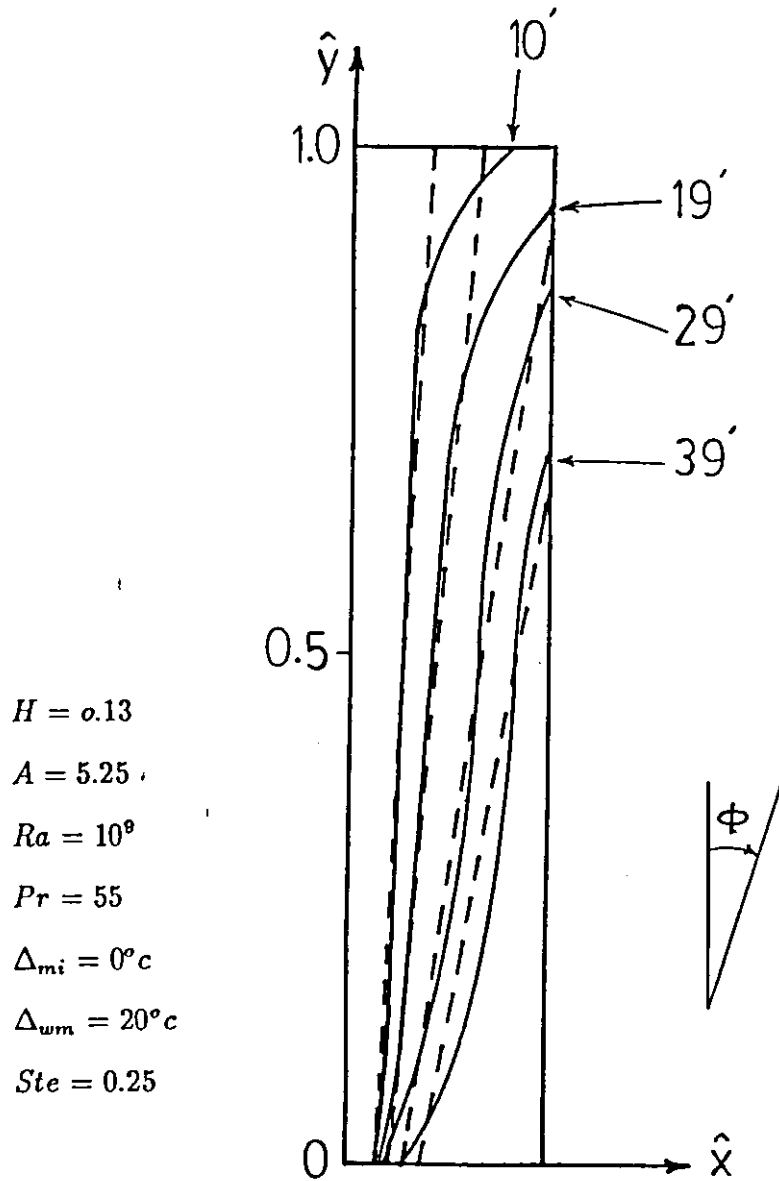
$\Delta_{wm} = 20^\circ c$

$Ste = 0.25$

Fig.5.5 Time evolution of the solid-liquid interface and its inclination angle. Results of this work (- - -). Numerical results of [44](——).

5.3   The Melted Fraction Of PCM

In this section, experimental and numerical matrixes used in selected previous works will be substituted in the concerned developed analytical equations of this work, specifically equations (4-41), (4-44), (4-45), (4-47), (4-50) and (4-51), thus, the values of $\hat{S}_0$, $\hat{\phi}$, F_b and F_a will be determined at the same times used in the previous works. The obtained results will be compared against the experimental and numerical results of the previous works.

The time evolution of the melted fraction obtained experimentally by Benard et al [15] is displayed in Fig.5.6. The employed model is a rectangular experimental cell filled with n-octadecane paraffin wax. Experimental results were obtained using photographic observations and the corresponding matrix is substituted in the developed equations of this work. Results of this work are obtained and plotted in the same figure which shows well agreement between these results and the experimental results. However, the rate of melting obtained in this work is slightly higher than the rate obtained experimentally. This is due to the actual heat loss across the experimental cell walls.

The numerical study results obtained by Webb et al [54] are shown in Fig.5.7. The employed model in this example is a rectangular enclosure filled with pure gallium metal. The numerical matrix is substituted in the developed equations of this work. Results are obtained and displayed in the same figure. The values of the melted fraction obtained in this work are found to be about 16% higher than the numerical study results. This difference could be due to the anisotropic thermal conductivity and the high thermal diffusivity of the pure gallium which caused a 60% melting fraction after only 20 minutes. These matters were taken in account in the numerical study. For comparison, the conduction-controlled melting rate obtained by [54] is displayed in the figure which shows that it is much slower than the other two rates.

The effect of the aspect ratio on the melted fraction was investigated numerically by Yeung [55] by employing three rectangular enclosures of different values of aspect ratio and the same width, containing n- octadecane as a test PCM. The numerical

results are displayed in Fig.5.8a which shows that the smaller enclosure was of the

highest melted fraction. The three enclosures are shown schematically in Fig.5.9. The numerical matrix of [55] is substituted in the developed equations of this work. Results are obtained and plotted in Fig.5.8b which shows that the smallest enclosure is of the highest melted fraction, which agree well with the numerical study results. It can be evaluated from figures 5.9a and 5.9b that the melting fraction after one hour of the melting process equals to 94%, 93% and 91% for the smallest, the middle and the largest enclosures respectively. Thus, it can be concluded that for the same enclosure width, temperature of the vertical isothermal heated wall and Stefan number, the efficiency of the enclosure of the smallest aspect ratio is slightly higher than that of the larger ones. The probable reason for this result is that the smallest enclosure is of the largest value of ϕ_B and accordingly the largest inclination of the solid-liquid interface which decreases the velocity, v_c, of the liquid particles inside the cold boundary layer allowing for longer heat transfer time between these particles and the interface and slightly more melted fraction is attained. This conclusion would be useful to apply in PCES systems where a thermal storage wall of specified depth may be made up from several identical PCM-filled enclosures stocked on top of each other. But, on the other hand, there are economical limits for that because a larger enclosure may cost less than several smaller ones knowing that the gain in the efficiency does not exceed 5%. In the practical applications, the availability of isothermal heated walls is of less probability compared to that of walls subject to constant heat flux.

5.4 Effects Of *Ste*, *Nu* And *Pr* Numbers And The Enclosure Height On The Melting Process

The average values of *Nu* number which are obtained using equations (4-54) and (4-57) are compared against experimental and numerical results of previous works. Experimental results obtained by Buren et al [13] are shown in Fig.5.10 in which it is found that the average *Nu* number obtained in this work can be considered an average for the experimental results. The variation of *Nu* number with the altitude

was found numerically by Okada [35] as shown in Fig.5.11. The average value of

Nu number obtained in this work is plotted in the same figure. As shown in figure, it can be considered as an average for these numerical results. Thus, concerning Nu numbers, the results obtained in this work agree with experimental and numerical results.

In order to demonstrate the effects of Ste and Pr numbers and the enclosure height, H, on the melting process, the dimensional average heat flux supplied to the vertical isothermal heated wall of the enclosure is evaluated from equation (4-52) as

$$(q_w)_{av} = \frac{1}{H}[0.543 k_l \Delta_{wm} (Ra)^{1/4}] \tag{5.1}$$

Using this equation, the following dimensional relationships are evaluated:

- For fixed value of H:

$$(q_w)_{av} \propto (Ste)^{5/4} \tag{5.2}$$

- For fixed value of Ste number:

$$(q_w)_{av} \propto (H)^{-1/4} \tag{5.3}$$

- For fixed values of H and Ste number:

$$(q_w)_{av} \propto (Pr)^{1/4} \tag{5.4}$$

In order to investigate numerically the effects of the variation of the above parameters, the experimental matrix of the first example in section 5.2 is substituted in the above developed equations. From the obtained results, it is found that a value of $621 W/m^2$ as average heat flux is required to maintain the isothermal level of the vertical heated wall at $37°c$ while running the melting process. If Ste number is doubled, T_w value will be $46°c$ and the required average heat flux should be 1475 W/m^2. Thus, for a raise of $9°c$ in the isothermal level, the average heat flux should be increased by 138% which indicates to the great effect of Ste number while the value of H is kept constant. On the other hand, it is found for the same example that for an increment of 25% in Pr number, the heat flux should be increased by

only 5%, and for a increment of 25% in the height, H, of the enclosure, the heat flux should be decreased by 5% only. Thus, the melting process is much more dependent on Ste number than its dependence on Pr number and the enclosure height.

H	A	Ra	Ste	Pr	T_m	Δ_{wm}	Δ_{mi}
0.175	2.54	10^9	0.084	54	$28^\circ c$	$9^\circ c$	$0^\circ c$
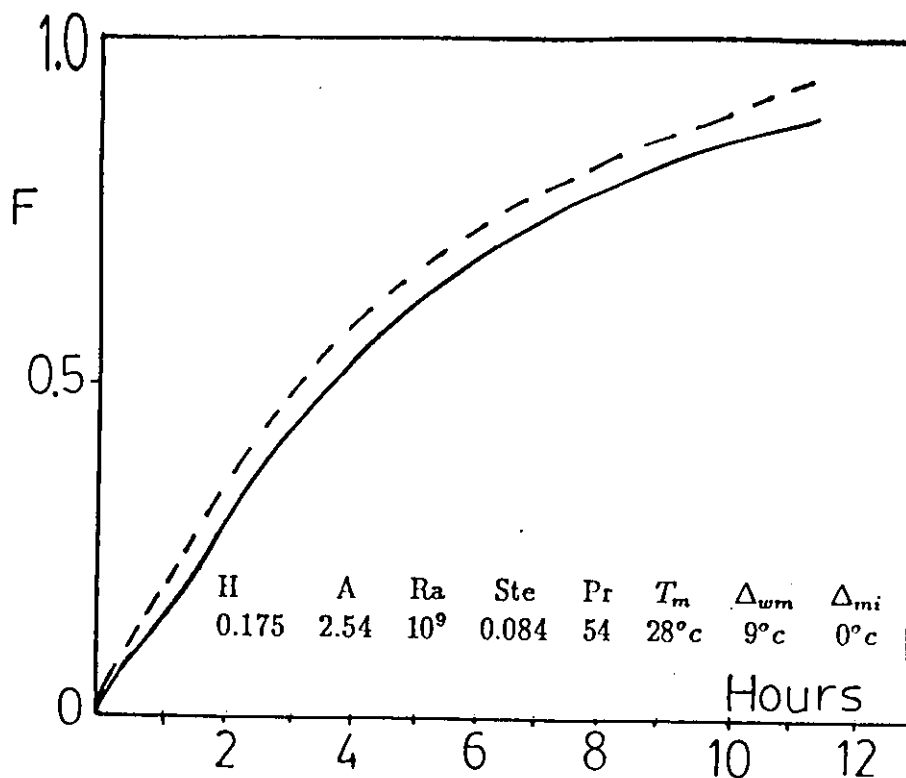
Fig.5.6 Melted fraction of n-octadecane. (- - -) results of this work. (—) results of experimental work [15].

Ra	Ste	Pr	T_m	Δ_{wm}	Δ_{mi}	α/H^2
2.2×10^5	0.042	0.021	$8^\circ c$	$0^\circ c$	$0^\circ c$	0.004
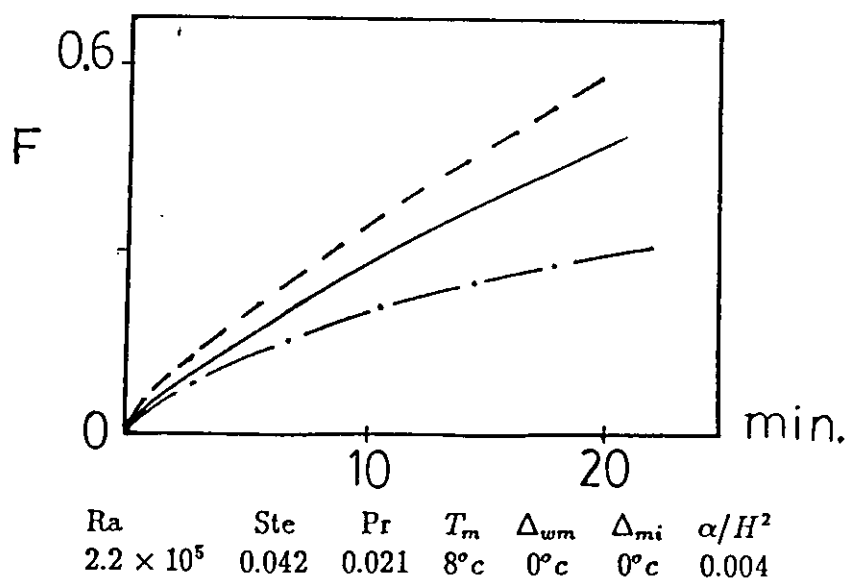
Fig.5.7 Melted fraction of pure gallium. (- - -) this work. (—) numerical [54]. For comparison, the conduction mode of heat transfer is displayed (- - -) by [54].
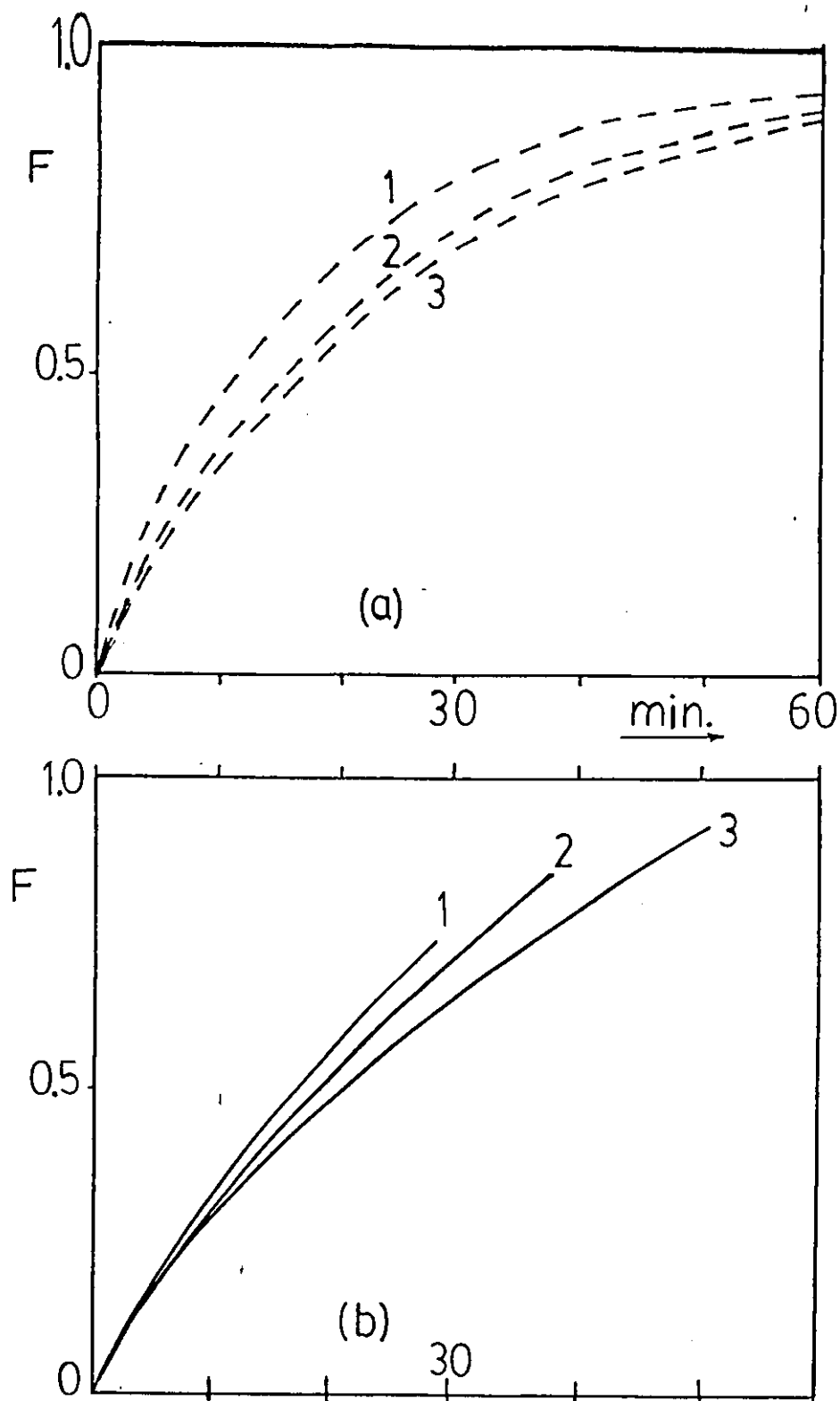
Fig.5.8 Melted fraction of n-octadecane in the three enclosures (shown in Fig.5.9a).

(a) This work (- - -). (b) Numerical work [55] (—).
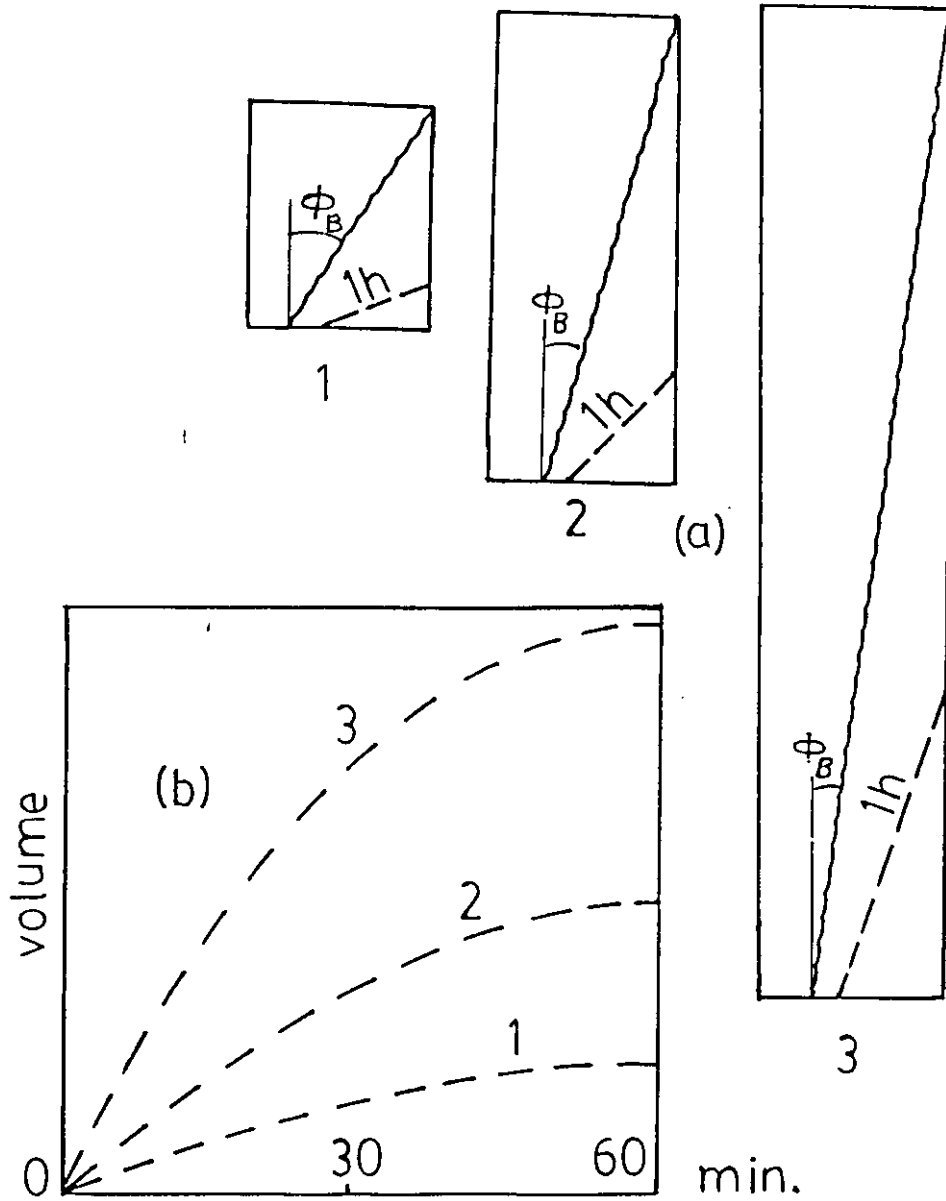
	A	Ra	H	Δ_{wm}	Δ_{mi}	Pr	Results
Enclosure 1 :	1.13	10^7	0.028m	$22^\circ c$	$0^\circ c$	50	$\phi_b = 31^\circ c$
Enclosure 2 :	2.44	10^8	0.061m	$22^\circ c$	$0^\circ c$	50	$\phi_b = 16^\circ c$
Enclosure 3 :	5.25	10^9	0.131m	$22^\circ c$	$0^\circ c$	50	$\phi_b = 8^\circ c$

Fig.5.9 (a) Schematic elevations of three enclosures containing n-octadecane as test PCM and heated from vertical isothermal sides. The melted fraction for the angle ϕ_B and after 1hr is shown. (b) A comparison between the absolute volumetric melting rates of the three enclosures.
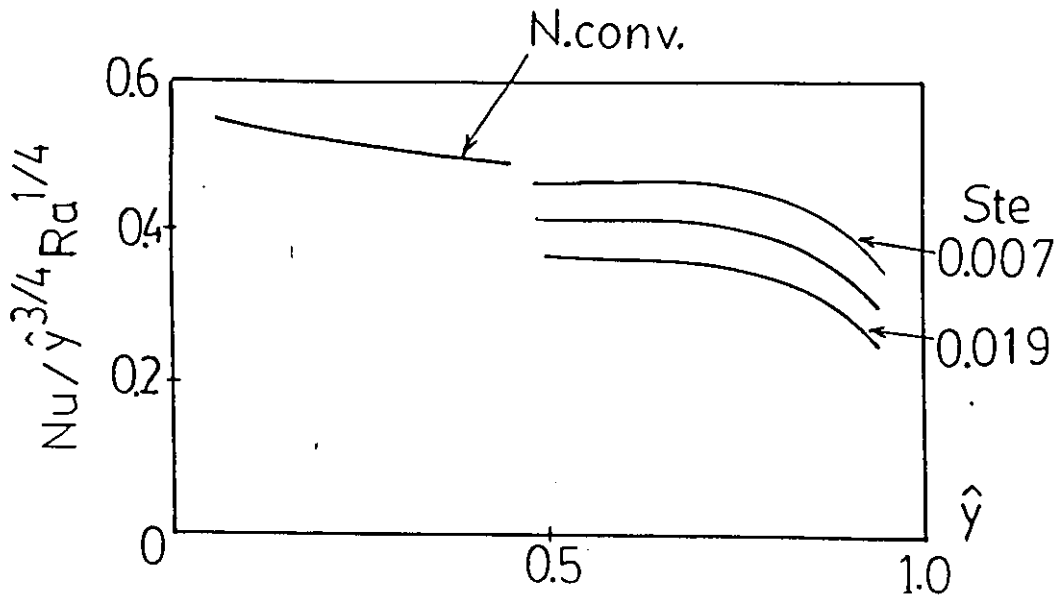
Fig.5.10 .Effect of H, *Ste* and y on the dimensionless parameter $Nu/(y^3 Ra)^{1/4}$ during melting of n-heptadecane paraffin wax [13].

Fig.5.11 The average value of *Nu* number. (- - -) this work. (—) numerical results of [35].

5.5 Thermal Energy Storage Rate

In the previous examples, the results obtained in this work for the dependent parameters of the melting process have been of well agreement with the results obtained in selected experimental and numerical previous works. This is an indication to the satisfactory efficiency of the analytical solution developed in this work. Thus, it can be stated with confidence that 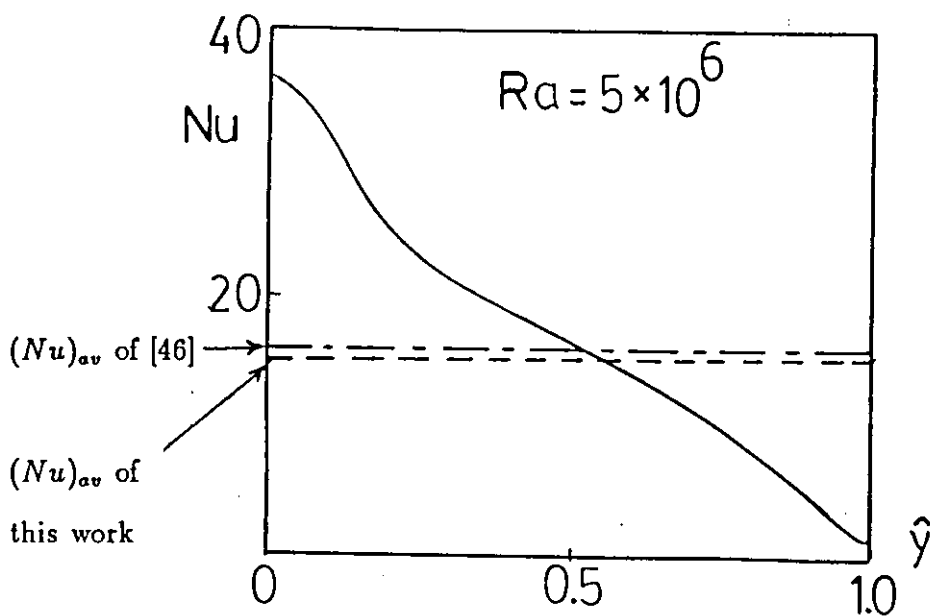this solution can be employed to predict the experimental data to a sufficient degree of accuracy which is comparable to that of the numerical methods. Accordingly, the analytical solution developed in this work is applied in this section to predict the amount of the thermal energy that may be stored within an enclosure filled with a PCM. Unfortunately, there is no experimental data available to be used for comparison, but, as stated above, this analytical solution may be used with confidence.

It can be excluded from the previous sections that to maintain the temperature of the vertical heated wall of the enclosure at a certain isothermal level while running the melting process, the heat supply at the outer surface of the wall should be of its maximum value at the bottom of the wall then it should decrease in a proportional relationship to altitude, $\hat{y}$, until being of zero value at the top of the wall (at $\hat{y} = 1$). This statement can be formulated in a mathematical relationship which can be obtained by using equations (4-27) and (4-28) to give

$$q_w(\hat{y}) \propto (1 - \hat{y}^{3/2})/\hat{y}^{1/4} \qquad (5.5)$$

On the other hand, the average heat supply, $(q_w)_{av}$, can be employed instead of this relationship for the corresponding study in this section. In the practical applications, the value of $(q_w)_{av}$ depends essentially on the availability of the heat flux at the outer surface of the wall. Sometimes, this heat flux is dependent on external circumstances as in the case of the solar heat irradiation which is available for a limited duration and at certain values. In order to approach into applications of solar energy systems, a heat flux of a value of 620 W/m^2 is proposed as the available average heat supply in the following example.

To investigate the amount of thermal energy storage using the analytical solution

developed in this work, two rectangular enclosures are proposed, a large and a smaller one (referred to as 1 and 2). Each enclosure is filled with n-octadecane paraffin wax as a PCM, and is being heated from a vertical isothermal wall. while all the other walls of the enclosure are insulated. The two proposed enclosures and their corresponding informations matrixes are shown in Fig.5.12. . The available average heat flux supplied at the outer surface of the wall is assumed to be of a value of 620 W/m^2 for a duration of 8 hours. Considering that $(q_w)_{av}$ is of the same value of the heat flux and substituting the informations matrix of each enclosure in equation (5-1), the temperatures of the heated wall and Ste and Ra numbers are evaluated to be

$$T_1 = 37^\circ c, \qquad (Ste)_1 = 0.084, \qquad (Ra)_1 = 10^9$$

$$T_2 = 38.9^\circ c, \qquad (Ste)_1 = 0.101, \qquad (Ra)_2 = 2.05 \times 10^{10}$$

In the most thermal storage applications, and consequently in the most experimental investigations of the problems of melting in a rectangular enclosure, Ra number is found to be of high values, typically in the range of $10^9 \leq Ra \leq 10^6$ [11,12,35,37,44]. Experimental evidences indicate that the liquid flow in such problems remains entirely laminar for this range of Ra numbers. Transition to turbulence occurs only for Ra numbers of values beyond 10^{10} [15,44]. Ra number of the liquid flow inside the larger enclosure is found to be of a value slightly higher than 10^{10}. Despite of that, it is assumed in this example that the liquid flow is still laminar [9,18]. The thermal energy which is stored inside each rectangular consists of two contributions:

- Sensible heat gain, $G_{sensible}$

- Latent heat gain, G_{latent}

Using equations (4-33), (4-41), (4-44), (4-47), (4-50) and (4-51) and performing the required integrations, sensible and latent heat storage equations are developed and added together to form general equations for the total heat gain (which equals to the summation of the sensible and latent heat) as in the following dimensionless equations

$$(\hat{G}_t)_b = (1 + 0.4Ste)\hat{S}_0 + (0.5 + 0.29Ste)Ra^{1/5}(tan\phi) \qquad (5.6)$$

$$(\hat{G}_t)_a = Ra^{1/5}[\frac{1}{A}(1 + 0.4Ste) - J^2(tan\phi)(0.5 + 0.11J^{2/3})] \qquad (5.7)$$

Where

$$J = (Ra^{1/5} - A\hat{S}_0)/(ARa^{1/5}tan\phi) \qquad (5.8)$$

$$\hat{G} = GRa^{1/5}/H^2\rho_l Q_{sl} \qquad (5.9)$$

Noting that the symbol J is introduced to simplify these equations which represent the total the total energy gain which is stored in the enclosure. These equations are dependent on *Ste*, *Pr* and *Ra* numbers in addition to the temporal values of $\hat{S}_0$ and ϕ.

Equations (4-41), (4-44), (4-45) and (4-47) are used to evaluate the values of $\hat{S}_0$ and ϕ at certain times. From the obtained values of ϕ, the value of ϕ_B is determined, by using equation (4-48), for each enclosure. The informations matrix of each enclosure is substituted in equations (5-2), (5-3), (5-4) and (5-5), then, obtained values of $\hat{S}_0$ and ϕ are used to evaluate $\hat{G}_t$ for each enclosure at the corresponding times.

Finally, using the values of $\hat{G}_t$, the specific heat gain values (in terms of MJ/m^2) are found and plotted against time as shown in Fig.5.12 for both of the enclosures. The specific heat gain is defined here as the amount of thermal energy which can be stored in the enclosure per the unit area of its vertical isothermal heated wall.

As shown in the figure, the specific heat gain in the large enclosure is about 19% more than than that in the small one. Thus, for a certain value of heat flux available at the outer surface of the wall of enclosures, it is more efficient to employ enclosures of larger heights while the corresponding *Ra* number is kept in the laminar range. Yhe percentage of the contribution in the TES amount is about 95% for the latent heat and 5% for the sensible heat. At the end of the 8 hours duration, the efficiency of the large and small enclosures are found to be about 79% and 62% respectively, noting that this efficiency is defined as the ratio between the specific heat gain and the specific hat flux available at the outer surface of the enclosure.
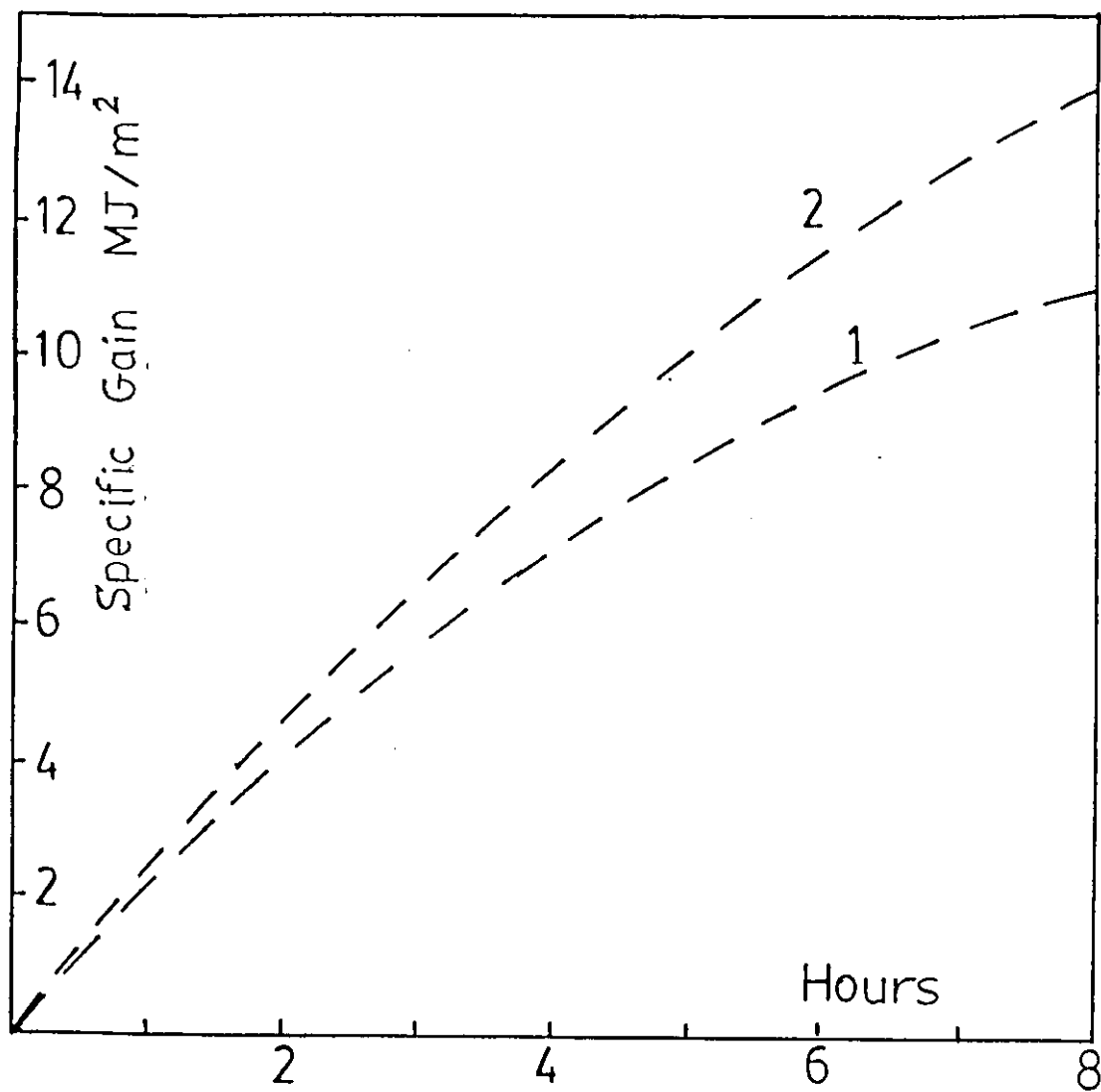
	Ra	Ste	Pr	T_m	T_w	H	A	$(q_w)_{av}$
	-	-	-	c^o	c^o	m	-	W/m^2
Enclosure 1 :	10^9	0.084	54	28	37	0.175	2.54	620
Enclosure 2 :	$2(10)^{10}$	0.101	54	28	39	0.45	2.54	620

Fig.5.12 Time evolution for the specific TES for two enclosures of different heights. Results are obtained by this work.

Chapter 6

CONCLUSIONS AND RECOMMENDATIONS

6.1   Conclusions

This work has conveyed analytical investigation on phase change problems involving melting of PCM contained in rectangular enclosure heated from isothermal vertical wall. Analytical solution is developed and employed to be used in easy, simple and quick procedure to predict, at any required time, the corresponding parameters of the melting process such as the position and inclination of the solid-liquid interface, the fraction of the melted PCM and the amount of TES within the enclosure. The motivating objectives, discussed in chapter I, has been covered and achieved in this work.

The conclusions which has been obtained in this work can be summarized as follows:

1. Analytical solution can be developed for a complex problem such as melting inside a rectangular enclosure with a satisfactory degree of accuracy and efficiency despite of the avoidance of the majority of the previous works such type of solution.

2. Results of this work have been of good agreement with experimental and numerical results which indicates that the natural convection, which has been taken into account in this work, is the predominant mode of heat transfer in the melting process.

3. The most important characteristics of natural convection mode of heat transfer

has been found to be the thermal stratification of the liquid core and the vortical motion of the liquid particles between the two boundary layers around the relatively stationary liquid core.

4. Conduction mode of heat transfer, which controls the melting process at early stages, does not ebb completely after that as was considered by other previous works, but it continues in controlling the melt propagation at the bottom of the enclosure until the end of the melting process. This fact was approved because the results of this work, concerning propagation of the melt layer at the bottom were of good agreement with experimental and numerical works.

6.2   Recommendations

As the analytical solution developed in this work has been found of satisfactory accuracy, thus, it is recommended to:

- Develop similar analytical solutions for:

  1. Other configurations like the cylindrical ones.

  2. Inclined rectangular enclosures heated from above at constant heating rate.

  3. Solidification process of PCM.

- Investigate a PCES system using paraffin wax and to compare it with sensible TES systems.

LIST OF REFERENCES

[1] D. J. Morrison and I. Abdel-Khalik, "Effects Of Phase- Change Energy Storage On The Performance Of Air-Based And Liquid-Based Solar Heating Systems," Solar Energy, Vol. 20, pp. 57-67, 1978.

[2] R. H. Henze and J. Humphery, "Enhanced Heat Conduction In Phase-Change Thermal Energy Storage Devices,' Int. J. Heat Mass Transfer, Vol. 24, pp. 459-474, 1981.

[3] A. D. Soloman, "Melt Time And Heat Flux For A Simple PCM Body," Solar Energy, Vol. 22, pp. 251-257, 1979.

[4] A. G. Bathelt and R. Viskanta, "Heat Transfer At The Solid-Liquid Interface During Melting From A Horizontal Cylinder," Int. J. Heat Mass Transfer, Vol. 23, pp. 1493-1503, 1980.

[5] C. Benard and D. Gobin, "Experimental Results Of A Latent- Heat Solar-Roof, Used For Breeding Chickens," Solar Energy, Vol. 26, pp. 347-359, 1981.

[6] R. Marshall and C. Dietsche, "Comparisons Of Paraffin Wax Storage Subsystem Models Using Liquid Heat Transfer Data," Solar Energy, Vol. 29, pp. 503-511, 1982

[7] C. J. Ho and R. Viskanta, "Heat TRansfer During Melting From An Isothermal Vertical Wall," Journal Of Heat Transfer, Vol. 106, pp. 12-19, 1984

[8] J. Eftekhar and A. Haji-Sheikh, " Heat TRansfer Enhancement In A Paraffin Wax Thermal Storage System," Journal Of Solar Energy Engineering, Vol. 106, pp. 299-306, 1984.

[9] Z. Zhang and A. Bejan, "Melting In An Enclosure Heated At Constant Rate," Int. J. Heat Mass Transfer, Vol. 32, pp. 1063- 1076, 1989.

[10] R. Marshal, "Parametric Sensitivity Studies Using Paraffin Wax Storage Sub-Systems," Solar Energy, Vol. 32, pp. 41-48, 1984.

[11] E. M. Sparrow, R. R. Schmidt and J. W. Ramsey, "Experiments On The Pole Of Natural Convection," Journal Of Heat Transfer, Vol. 100, pp. 11-16, 1978.

[12] N. W. Hale and R. Viskanta, "Photographic Observations Of The Solid-Liquid Interface Motion During Melting Of A Solid Heated From An Isothermal Vertical Wall," Letters In Heat And Mass Transfer, Vol. 5, pp. 329-337, 1978.

[13] P. D. Van Buren and R. Viskanta, "International Measurements Of Heat Transfer During Melting From A Vertical Surface," Int. J. Heat Mass Transfer, Vol. 23, pp. 568-571, 1980.

[14] E. M. Sparrow, J. W. Ramsey and J. S. Harris, "The Transition From Natural-Convection-Controlled Freezing To Conduction- Controlled Freezing," Journal Of Heat Transfer, Vol. 103, pp. 7-12, 1981.

[15] C. Benard, G. Gobin and F. Martinez, "Melting In Rectangular Enclosures: Experiments And Numerical Simulations," Journal Of Heat Transfer, Vol. 107, pp. 794-802, 1985.

[16] B. W. Webb and R. Viskanta, "Natural-Convection-Dominated Melting Heat Transfer In An Inclined Rectangular Enclosure," Int. J. Heat Mass Transfer, Vol. 29, pp. 183-192, 1986.

[17] C. Gau and R. Viskanta, " Melting And Solidification Of A Pure Metal On A Vertical Wall," Journal Of Heat Transfer, Vol. 108, pp. 174-181, 1986.

[18] Z. Zhang and A. Bejan, "The Problem Of Time-Dependent Natural Convection Melting With Conduction In The Solid," Int. J. Heat Mass Transfer, Vol. 32, pp. 2447-2457, 1989.

[19] Z. Zhang and A. Bejan, "Solidification In The Presence Of High Rayleigh Number Convection In An Enclosure Cooled From The Side," Int. J. Heat Mass transfer, Vol. 33, pp. 661-671, 1990.

[20] M. N. Ozisik, "Heat Conduction," John Wiley And Sons, N.Y., 1980.

[21] R. S. Gupta and D. Kumar, "Variable Time Step Methods For One-Dimensional Stefan Problem With Mixed Boundary Condition," underlineInt. J. Heat Mass Transfer, Vol. 24, pp. 251-259, 1981.

[22] E. R. G. Eckert, "Analysis Of Heat And Mass Transfer," McGraw-Hill Kogakusha Ltd., Tokyo, 1972.

[23] N. V. Tsederberg, "Thermal Conductivity," Edward Arnold Publishers Ltd., London, 1965.

[24] G. E. Myers, "Analytical Methods In Conduction Heat Transfer," McGraw-Hill Book Company, USA, 1971.

[25] E. A. Krasnnoshchekov, "Problems In Heat Transfer," Mir Publishers, Moscow, 1975.

[26] J. P. Holman, "Heat Transfer," McGraw-Hill Kogakusha Ltd., Tokyo, 1976.

[27] S. S. Kutateladze, "A Concise Encyclopedia Of Heat Transfer," Pergamon Press Ltd., London, 1966.

[28] A. J. Ede, "An Introduction To Heat Transfer," Pergamon Press Ltd., London, 1967.

[29] F. Kreith, "Basic Heat Transfer," Harper And Row, Publishers, N.Y., 1980.

[30] F. P. Increpera, "Fundamentals Of Heat Transfer," John Wiley And Sons, N.Y., 1981.

[31] L. C. Burmeister, "Convective Heat Transfer," McGraw-Hill Book Company, N.Y., 1982.

[32] M. N. Ozisik, "Basic Heal Transfer," McGraw- Hill Kogakusha, Tokyo, 1977.

[33] T. Hirata and K. Nishida, "An Analysis Of Heat Transfer Using Equivalent Thermal Conductivity Of Liquid Phase During Melting Inside An Isothermally Heated Horizontal Cylinder," Int. J. Heat Mass Transfer, Vol. 32, pp. 1063-1076, 1989.

[34] C. Benard, Y. Body and D. Gobin, " Use Of A Variable Parameter Test-Cell For The Study Of Latent-Heat Solar Walls," Solar Energy, Vol. 29, pp. 101-109, 1982.

[35] M. Okada, "Analysis Of Heat Transfer During Melting From A Vertical Wall," Int. J. Heat Mass Transfer, Vol. 27, pp. 2057- 2066, 1984.

[36] S. Aboul-Enien and M. R. I. Ramadan, "Storage Of Low Temperature Heat In Salt-Hydrate Melts For Heating Applications," Solar And Wind Technology, Vol. 5, pp. 441-444, 1988.

[37] E. M. Sparrow, S. V. Patanker and S. Ramadhyani, "Analysis Of Melting In The Presence Of Natural Convection In The Melt Region," Jornal Of Heat Transfer, Vol. 99, pp. 520-526, 1977.

[38] L. E. Goodrich, "Efficient Numerical Technique For One- Dimensional Thermal Problems With Phase Change," Int. J. Heat Mass Transfer, Vol. 21, pp. 615-621, 1978.

[39] T. Saitoh,"Numerical Method For The Multi-Dimensional Freezing Problems In Arbitrary Domains," Journal Of Heat Transfer, Vol. 100, pp. 294-299, 1978.

[40] B. Rubinsky and E. Cravahlo, "A Finite Element Method For The Solution Of One-Dimensional Phase Change Problems," Int . J. Heat Mass Transfer, Vol. 24, No. 12, pp. 1987-1989, 1981.

[41] T. R. Hsu and G. Pizey, "On The Prediction Of Fusion Rate Of Ice By Finite Element Analysis," Journal Of Heat Transfer, Vol . 103, pp. 727-732, 1981.

[42] C. F. HSU and E. M. Sparrow, "Numerical Solution Of Moving Boundary Problems By Boundary Immobilization And A Control-Volume-Based Finite-Difference Scheme," Int. J. Heat Mass Transfer, Vol. 24 , No. 8, pp. 1335-1343, 1981.

[43] T. Saitoh and H. Hirose, "High Rayleigh Number Solutions To Problems Of Latent Heat Thermal Energy Storage In A Horizontal Cylindrical Capsule," Journal Of Heat Transfer, Vol. 104, pp. 545-553, 1982.

[44] A. Gadgil and D. Gobin, " Analysis Of Two-Dimensional Melting In Rectangular Enclosures In Presence Of Convection," Journal Of Heat Transfer, Vol. 106, pp. 20-26, 1984.

[45] P. R. Roa and V. Sastri, "Efficient Numerical Method For Two- Dimensional Phase Change Problems," Int. J. Heat Mass Transfer , Vol. 27, pp. 2077-2084, 1984.

[46] M. A. Katz and B. Rubinsky, "An Inverse Finite-Element TEchnique To Determine The Change Of Phase Interface Location In One- Dimensional Melting Problems," Numerical Heat TRansfer, Vol. 7 , pp. 269-283, 1984.

[47] A. T. Patera, "A Finite-Element/Green's Function Embedding Technique Applied To One-Dimensional Change-Of-Phase Heat Transfer," Numerical Heat Transfer, Vol. 7, p. 241-247, 1984.

[48] Q. T. Pham, "A Fast Unconditionally Stable Finite-Difference Scheme For Heat Conduction With Phase Change," Int. J. Heat Mass Transfer, Vol.28, pp. 2079-2084, 1985.

[49] Q. T. Pham, "The Use Of Lumped Capacitance In The Finite-Element Solution Of Heat Conduction Problems With Phase Change," Int. J. Heat Mass Transfer, Vol. 29, pp. 285-291, 1986.

[50] J. Menning and M. N. Ozisik, "Coupled Integral Equation Approach For Solving Melting Or Solidification," Int. J. Heat Mass Transfer, Vol. 28, pp. 1481-1485, 1985.

[51] Ch. Charch and P. B. Khan, "Solidification In Finite Bodies With Prescribed Heat Flux: Bounds For The Freezing Time And Removed Energy," Int. J. Heat Mass Transfer, Vol. 30, pp. 233-240, 1987.

[52] H. Chen, "Application Of Laplace Transform/Finite-Difference Method To Transient Heat Conduction Problems," Numerical Heat Transfer, Vol. 14, pp. 343-356, 1988.

[53] S. D. Gilmore, "Three-Dimensional Solidification, A Numerical Approach," Numerical Heat Transfer, Vol. 14, pp. 165 -186, 1988.

[54] B. W. Webb and R. Viskanta, "Analysis Of Heat Transfer During Melting Of A Pure Metal From An Isothermal Vertical Wall," Numerical Heat Transfer, Vol. 9, pp. 539-558, 1986.

[55] W. S. Yeung, "Engineering Analysis Of Heat Transfer During Melting In Vertical Rectangular Enclosures," Int. J. Heat Mass Transfer, Vol. 32, pp. 689-696, 1989.

[56] W. Shyy and M. Chen, "Steady State Natural Convection With Phase Change," Int. J. Heat Mass Transfer, Vol. 33, pp. 2545- 2563, 1990.

[57] C. Kim and M. Kaviany, "A Numerical Method For Phase-Change Problems," Int. J. Heat Mass Transfer, Vol. 33, pp. 2721-2734, 1990.

[58] B. Vujanovic, "Application Of Optimal Linearization Method To The Heat Transfer Problem," Int. J. Heat Mass Transfer, Vol. 116, pp. 1111-1117, 1973.

[59] A. Aziz and J. Y. Benzies, "Application Of Perturbation Techniques To Heat Transfer Problems With Variable Thermal Properties," Int. J. Heat Mass Transfer, Vol. 19, pp. 271-276, 1976.

[60] B. Vujanovic and B. Baclic, "Applications Of Gauss Principle Of Least Constraint To The Nonlinear Heat Transfer Problem," Int. J. Heat Mass Transfer, Vol. 19, pp. 721-730, 1976.

[61] S. Weinbaum and L. M. Jiji, "Singular Perturbation Theory For Melting Or Freezing In Finite Domains Initially Not At The Fusion Temperature," Journal Of Applied Mechanics, pp. 25-30, March, 1977.

[62] B. Rubinsky and A. Shitzer, "Analytic Solutions To The Heat Equation Involving A Moving Boundary With Applications To The Change Of Phase Problem (The Inverse Stefan Priblem), Journal Of Heat Transfer, Vol. 100, pp. 300-304, 1978.

[63] N. Ramachandran, Y. Jaluria and J. P. Gupta, "Thermal And Fluid Flow Characteristics In One-Dimensional Solution," Letters In Heat And Mass Transfer, Vol. 8, pp. 69-77, 1981.

[64] A. D. Soloman, "On The Limitations Of Analytical Approximations For Phase Change Problems With Large Biot Numbers," underlineLetters In Heat And Mass Transfer, Vol. 8, pp. 475-482, 1981.

[65] A. M. C. Chan, P. Smereka and M. Shoukri, "An Approximate Analytical Solution To The Freezing Problem Subject To Convective Cooling And With Arbitrary Initial Liquid Temperatures," Int. J. Heat Mass Transfer, Vol. 26, pp. 1712-1715, 1983.

424998

[66] Ch. Charach and P.Zogin, "Solidification In A Finite Initially Overheated Slab," Int. J. Heat Mass Transfer, Vol. 28, pp. 2261-2268, 1985.

[67] L. V. Gutman, "On The Problem Of Heat Transfer In Phase- Change Materials For Small Stefan Numbers," Int. J. Heat Mass Transfer, Vol. 29, pp. 921-926, 1986.

[68] M. Mashen and A. Haji-Sheikh, "An Integral Solution Of Moving Boundary Problems," Int. J. Heat Mass Transfer, Vol. 29 , pp. 317-329, 1986.

[69] N. Li and J. Barber, "Sinusoidal Perturbation Solutions For Planer Solidification," Int. J. Heat Mass Transfer, Vol. 32, pp. 935-941, 1989.

[70] D. Lecomte and J. C. Batsale, "A Suitable Approximate Solution Of Neumann's Problem," Int. J. Heat Mass Transfer, Vol. 34, pp. 894-897, 1991.

[71] D. R. Pitts, "Theory And Problems Of Heat Transfer," Schaum's Outline Series, McGraw-Hill Book Company, N.Y., 1977.

[72] W. M. Kays, "Convective Heat Transfer," McGraw- Hill Book Company, N.Y., 1980

[73] J. H. Lienhard, "A Heat Transfer Text Book," Prentice-Hall, Inc., New Jersey, 1981.

Appendix A

PHASE CHANGE MATERIALS

Phase change materials (PCMs) are those engineering materials which are specified by the following properties:

1. Large value of latent heat of fusion.

2. Melting temperature near ambient temperatures.

3. Harmless to human use.

4. Chemically stable.

5. Does not cause corrosion to metals of enclosures.

6. Cost effective availability.

Due to the above properties, PCM's are found to be suitable to be used in PCES systems as mentioned in chapter II and in studies of phase change problems involving melting and solidification processes.

The most notable of the PCM's is the paraffin wax which is a by-product of the petrochemical industry in form of different hydrocarbons, each is with different melting temperature. It is of relatively low thermal conductivity with a range between 0.16 and 0.24 W/mc^o for the solid phase and is around 0.2 W/mc^o for liquid phase [8]. In general, all types of paraffin wax are transparent to the visible radiation which is a desired property in PCM's because it enables the photographic observations to be recorded in experimental works of melting and solidification processes. There are many types of paraffin wax, each is of different thermophysical properties. Properties

of PCM's can be found in a design hand book published by Humphries and Griggs for NASA T. P. 1074, (Nov.1977). Paraffin waxes are like n-octadecane $(C_{13}H_{38})$ [2,3,4,15,33], Suntech P116 [8], SUNOCO's P116 [1], Shell 53/54°c [6] and other types [3,4,13,14] like n-heptadecane, n-eicosane, n-tetradecane and n-hexadecane. On the other hand, there are other types of PCMs except the paraffin waxes like Glauber salt [68]. Thermophysical properties of notable PCMs are listed in the following table. For comparison, properties of water and ice [4o,46,49] are added.

Table of thermophysical properties of notable PCMs:

Properties	units	$(PCM)_1$	$(PCM)_2$	$(PCM)_3$	$(PCM)_4$	(water/ice)
T_m	(c^o)	28	44	53	31.7	0
Q_{sl}	(KJ/Kg)	242	226	251	139.5	335
$(10)^3\beta$	$(1/c^o)$	0.95	2.1	-	-	0.18
c_l	(KJ/Kgc^o)	2.2	2.51	2.07	1.01	4.18
c_s	(KJ/Kgc^o)	2.2	-	3.5	0.54	2.25
k_l	(W/mc^o)	0.155	0.2	0.126	3.26	0.6
k_s	(W/mc^o)	0.19	-	0.231	1.92	2.21
ρ_l	(Kg/m^3)	780	770	780	1330	1000
ρ_s	(Kg/m^3)	850	-	860	1460	918
$(10)^6\nu$	(m^2/s)	4.8	3.7	4	-	1.4

Where:

$(PCM)_1$, $(PCM)_2$, $(PCM)_3$ and $(PCM)_4$ are symbols referring to n-octadecane, Suntech P116, Shell 53/54 and Glauber salt respectively.

....

....

....

.....

ملخص

عنوان الرساله :
طريقة تحليليه رياضيه جديده لحل مسائل بتغيير حالة المادة.

في رسالة الماجستير هذه، تمت دراسة تحليليه لمسألة تحول المـاده
من حالتهـا الصلبـه الـى حالتهـا السائله اثناء انصهارهـا داخـل وعـاء
منشوري قائم يتم تسخينه من احد سطوحه الجانبيه مـع ابقـاء جميـع
سطوحه الأخرى معزوله حراريا. وقد وجد ان الأنتقـال الحـراري داخـل
الوعاء الذي يؤدي لعملية الأنصهار يتم لفترة قصيره بواسطة التوصيل
الحراري ثم تكتمل بعد ذلك العملية بواسطة الحمل الحـراري. وقـد تـم
حل المعادلات الرياضيه وتم استنتاج حلول تحليليـه لهـذه المعـادلات ثـم
بمقارنة نتائج هـذه الحلـول مـع نتـائج الأبحـاث العمليـة والعدديـة وجـدت
متطابقـه الـى درجـة جيـدة وكافيـة لاستخدامها فـي تقدير موقـع وميـلان
السطح الفاصل بين طوري الماده المنصهره فـي اي وقـت وكذلك كميـة
الطاقه الحرارية المخزنه علـى شـكل حـرارة انصهـار وتـم ترشـيح مـادة
الشمع البرافيني للتطبيقات العملية لتخزين الطاقه الشمسيه بشكل مجد .